AD-A080 364 AIR FORCE INST OF TECH WRIGHT-PATTERSON AFB OH SCHOO--ETC F/G 7/4
ULTRAVIOLET ABSORPTION CROSS-SECTION OF MERCURIC BROMIDE.(U)
DEC 79 G L FRANTOM

UNCLASSIFIED AFIT/GEP/PH/79D-2 NL

1 OF 1
AD A080 364

END
DATE FILMED
3-80
DDC

AFIT/GEP/PH/79D-2

(6) ULTRAVIOLET ABSORPTION CROSS-SECTION OF MERCURIC BROMIDE

(9) Master's THESIS

(14) AFIT/GEP/PH/79D-2

(10) Gordon L. Frantom
2Lt USAF

(11) Dec 71 (12) 71

Approved for public release; distribution unlimited.

AFIT/GEP/PH/79D-2

ULTRAVIOLET ABSORPTION CROSS-SECTION OF MERCURIC BROMIDE

THESIS

Presented to the Faculty of the School of Engineering

of the Air Force Institute of Technology

Air University

in Partial Fulfillment of the

Requirements for the Degree of

Master of Science

by

Gordon L. Frantom, A.A., B.S.

2Lt USAF

Graduate Engineering Physics

December 1979

Preface

The mercuric bromide photodissociation laser has the potential of becoming an important laboratory tool because of its efficiency characteristics. But to build such a laser and to do so efficiently, one must know the photoabsorption characteristics of this material.

This thesis is devoted entirely to obtaining those photoabsorption characteristics. Great detail was taken in designing and assembling a system so that the information obtained would be accurate and repeatable.

In the way of acknowledgments, there are many people who need to be mentioned. Thanks go out to all the people who work in the Plasma Physics Division of the AFAPL, they always seemed to have the right piece of equipment when you needed it. Many thanks go to Dr. A. Garscadden and M. R. Stamm, their pointers made the results of this experiment clearer. To my thesis advisor, Dr. Peter Bletzinger, I must show my graditude. His many suggestions saved a great deal of time, both during and after the experimentation. I must give special thanks to Dennis Grosjean of Systems Research Laboratories. Without his expert help in electronic interfacings and vacuum techniques this work would have been a great deal harder for me. And, finally, thanks go out to my typist, Jill Rueger, for putting up with me and helping me meet the deadlines on time.

Contents

List of Figures

List of Figures

Abstract

This report is on the measurements of the ultraviolet absorption cross section of mercuric bromide ($HgBr_2$) from 175.0 nm to 325.0 nm and discusses the need for such measurements. The ultraviolet radiation wavelengths from a hydrogen discharge lamp were selected by a vacuum monochromator (0.25 nm resolution) and passed through an absorption cell, made of fused quartz, containing the $HgBr_2$. The experiments were conducted over the temperature range 110°C to 150°C corresponding to vapor pressures of 0.2 torr to 2.15 torr of the $HgBr_2$. The results of this study are compared with the results of previous studies and clears up several discrepancies concerning the value of the absorption cross section. It further measures the value of the cross section of an absorption band at 184 nm that was not previously available.

I. Introduction

Background

As the Department of Defense, and science in general, becomes more and more interested in lasers, more knowledge must be obtained on materials to determine if they are candidates for laser media. This candidacy requires not only the availability of laser action, but further requires stability in the media as well as a system that has an acceptable efficiency. It is also desirable, from a laboratory view, to have a medium that doesn't deteriorate rapidly. A promising group of molecules that appears to have these characteristics is the mercury halides, HgX (X stands for bromine, Br; Chlorine, Cl; or Iodine, I).

Lasing for a HgX molecule was first observed by J. H. Parks in April 1977 (Ref 1). In this experiment he produced HgCl ($B^2\Sigma_{\frac{1}{2}}^+$) molecules by e-beam excitation in a mixture of Hg vapors and CCl_4 vapors along with other buffer gasses. A green laser line at 557.6 nm was observed with a quantum efficiency of 8.6%. A few weeks after this first report Parks published another (Ref 2) in which he reported laser action on the $B^2\Sigma_{\frac{1}{2}}^+ \rightarrow X^2\Sigma_{\frac{1}{2}}^+$ band of mercury bromide, HgBr. In this experiment he produced the HgBr ($B^2\Sigma_{\frac{1}{2}}^+$) molecules the same way, but replaced the CCl_4 with HBr. Again, a green laser line at 501.8 nm was observed with a quantum efficiency of 9.5%.

Parks further stated in these reports that the efficiency was limited by the energy needed to produce Ar ions which in turn would give rise to the HgX molecules. He stated, if a discharge was used to pump the Hg* (6p) metastable levels directly, the efficiencies of the HgCl and HgBr lasers would be roughly 45% and 50% respectively. This shows that HgCl and HgBr

promise higher efficiencies than have been previously achieved for visible lasers.

In July 1977 J. Eden reported a second laser line for the HgCl (Ref 3). The new line, also green, is at 558.4 nm. In this experiment, like the experiment by Parks, an e-beam was introduced into a mixture of Hg vapors, CCl_4 or CCl_3 vapors, and various buffer gasses. The importance of this new laser line is that HgCl shows the tendency of being tunable, and, hence a valuable laboratory tool.

Multiple laser lines were demonstrated for HgBr in May 1977 by E. J. Schimitschek, J. E. Celto, and J. A. Trias (Ref 4). Six laser lines, all green, from 502.0 nm to 504.6 nm were observed in an experiment that differed a great deal from previous experiments. In this experiment the HgBr ($B^2\Sigma^+_{\frac{1}{2}}$) molecules were obtained by photodissociating mercuric bromide ($HgBr_2$) vapors with the 193 nm line from an ArF excimer laser. Maximum efficiency obtained was about 3.6% for the 502.0 nm line. The importance of this experiment was not only the observation of multiple laser lines, but, also, the introduction of a method of producing the HgBr molecules that is cyclic. When lasing had occurred, the fragments of the dissociated $HgBr_2$ molecule recombined to produce the parent molecule again. The process could then be repeated many times without loss of output energy. This, of course, makes this material even more interesting, since now it shows the tendency of yielding a closed laser that does not require replenishing of the medium.

Further work in this area was reported in December 1977 by E. J. Shimitschek and J. E. Celto (Ref 5). In this report the multiple laser lines of the HgBr molecule were studied again, only this time the dissociation of the $HgBr_2$ molecule was achieved by an electric discharge. They

went on to report that several laser lines from 442 nm to 444 nm were observed by photodissociating HgI_2 to produce HgI ($B^2\Sigma^+_{\frac{1}{2}}$) molecules in the same type of experiment that was used on $HgBr_2$ (Ref 4).

The electric discharge dissociation laser, like the photodissociation laser, for $HgBr_2$ showed no loss in output energy over many pulses. This supports the previous argument that the dissociation-recombination reactions are cyclic in this medium. Another point that makes these materials interesting is that the vibrational transitions corresponding to the B → X transition is $v' = 0$ to $v'' = 22$ or 23 (tentative assignment). This envokes further interest, since the lower laser level has a high vibrational number, and in turn will be rapidly depopulated due to vibrational relaxation in the ground state.

At the present time no work has been completed and published in which a $HgBr_2$ photodissociation laser has been made using a broad band photolytic pump. The photolytic pumps are desirable due to the absence of the problem of arcing, and it has been argued that the dissociation-recombination of $HgBr_2$, while using a photolytic pump, is cyclic. And the use of a broad band pump is desired over the use of a narrow band pump (another laser) because narrow band pumps are very inefficient. But to achieve the optimum efficiency for such a laser one must know the absorption characteristics of the medium.

Purpose

The purpose of this study is to experimentally measure the ultraviolet absorption cross section of mercuric bromide ($HgBr_2$).

Scope

This study will be of the ultraviolet absorption cross section of

$HgBr_2$ and will be done experimentally with as much detail as possible. It will not, however, take on the task of building and optimizing a workable photodissociation laser using $HgBr_2$; nor will it delve into the theoretical representations of the reactions and reaction rates.

Assumptions

There are only two basic assumptions to be made for this experiment. First, it will be assumed that all measurements will be taken when the $HgBr_2$ vapors are at thermal equilibrium. Then the vapor pressure can be computed as a function of temperature according to the following equation from the CRC handbook (Ref 6):

$$\log_{10}P = (-0.2185\ A/T) + B \qquad (1)$$

where,

P = Pressure in torr

T = Temperature in °K

A = Molar heat of vaporization
= 19072.7 cal/gm-mole (from 110°C to 235°C)

B = Constant = 10.18100

See Figure 1 for a graph of this curve for $HgBr_2$ in the temperature range of 110°C to 150°C, which will be the operating range for this experiment.

Second, it will be assumed that the dissociation-recombination reactions for $HgBr_2$ are cyclic. This assumption is supported by the work done by Schimitscheck, et. al. (Ref 4). As stated previously, they observed no loss in output energy over many pulses of the $HgBr_2$ photodissociation laser. This implies that there was no degradation of the medium.

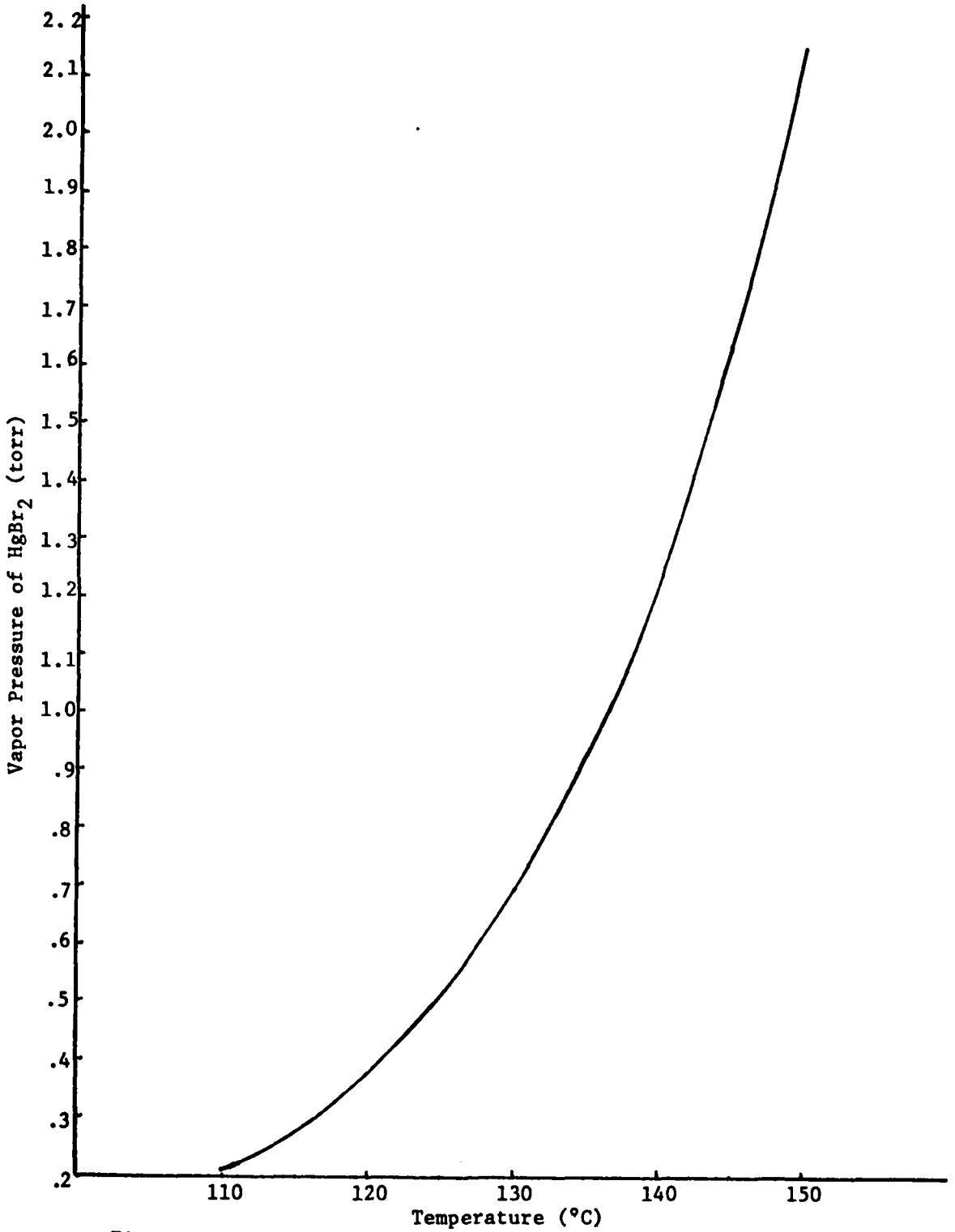

Figure 1: Vapor Pressure of $HgBr_2$ as a Function of Temperature

Using the second assumption along with an energy level diagram, Figure 2, the following conclusion can be drawn:

Radiation absorbed by the $HgBr_2$ vapors will excite the $HgBr_2$ molecules from a bound ground state (x-state) to higher excited states (a, b, c, etc.). These higher excited states appear to be dissociative, according to the broad absorption continua observed by Schimitschek and Celto (Ref 5), and Gedanken, et. al. (Ref 7), as well as several others. The first two excited states ("a" and "b") are dissociative, while the third excited state ("c"), due to its unresolved rotational structure (Gedanken, et. al.), is assumed to be predissociative. The absorption bands in the cross section that are due to excitation of $HgBr_2$ vapors into excited energy states are referred to as "a" band, "b" band, and so on depending on which $HgBr_2$ excited state is populated by absorption in that band. This is the notation commonly used for the mercuric halides, see Wieland (Ref 8).

The dissociations reactions can now be written, indicating the excited state of each molecule, by this notation, and the known reactions of metal halides and ultraviolet radiation (Ref 9). The absorption into the "a" band follows the reaction

$$HgBr_2(x) + h\nu_1 \rightarrow HgBr_2(a) \qquad (1)$$

$$HgBr_2(x) \rightarrow HgBr(X) + Br \qquad (2)$$

The absorption into the "b" band follows the reaction

$$HgBr_2(X) + h\nu_2 \rightarrow HgBr_2(b) \qquad (3)$$

$$HgBr_2(b) \rightarrow HgBr(B) + Br \qquad (4)$$

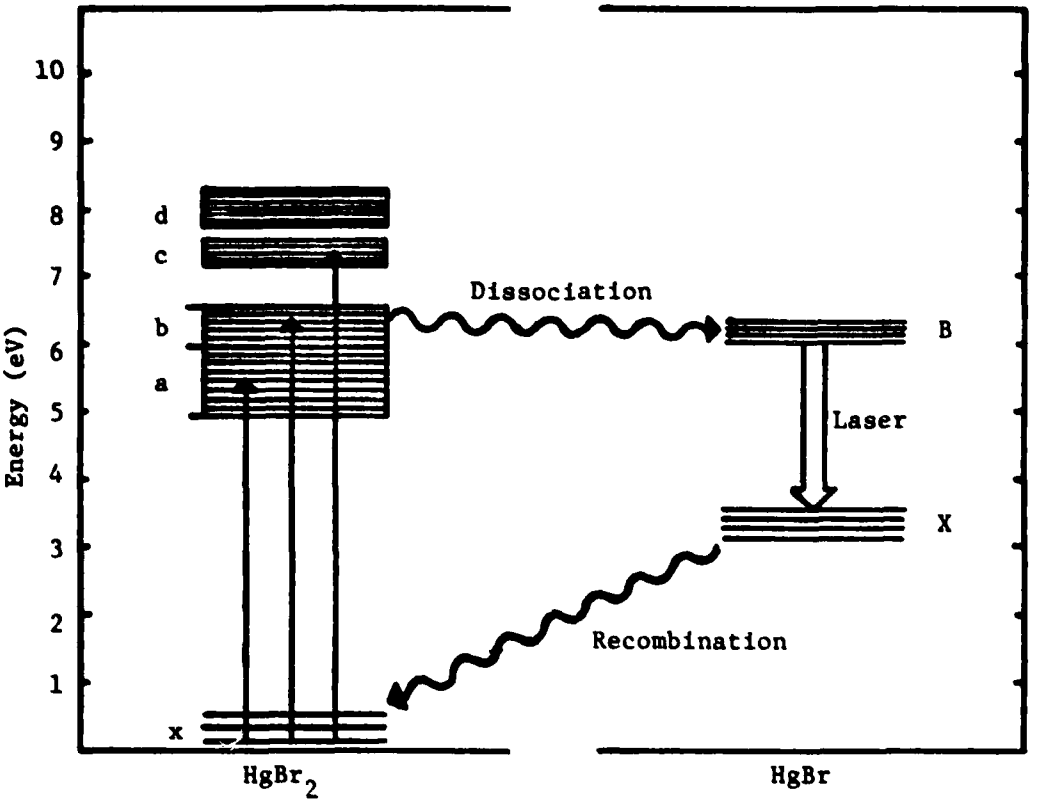

Figure 2; Energy level diagram (Ref 4).

The absorption into the "c" band follows the reaction

$$HgBr_2(x) + h\nu_3 \rightarrow HgBr_2(c) \quad (5)$$

$$HgBr_2(c) \rightarrow HgBr^* + Br \quad (6)$$

In equations 1, 3, and 5, $\nu_1 < \nu_2 < \nu_2$.

At the present time it is not known what excited state, for the HgBr, is populated by a dissociated $HgBr_2(c)$. Although, from the energy level diagram (see Figure 2) it can be seen that it is not a "B" state, should be a "C" state, but could possibly be a "D" state.

Summary of Current Knowledge

At the present time very little information is available on the ultraviolet absorption cross section of $HgBr_2$. Three experiments have been published but these three reports differ widely. See Figure 3 for a comparative graph of these three reports. This figure places all three reported absorption cross sections on the same scale, and it is easily seen that something is amiss. All three reports have the "a" and "b" absorption bands at about the same locations (~230 nm and 200 nm respectively), but they differ greatly in the value of the cross section. It should also be noted that none of these reports include a "c" absorption band which should be located at about 185 nm. The existence of this absorption band has been shown, for example see Gedanken, et.al. (Ref 7), but as of yet nobody has reported a value for the cross section of this band.

Looking at the other two mentioned mercuric halides, $HgCl_2$ and HgI_2, one finds the work here has yielded absorption cross sections showing all three bands on several occasions for the HgI_2, see Maya (Ref 10) and Templet, et. al. (Ref 11). This leads one to believe that a cross section measurement for $HgBr_2$ could be made that shows, and assigns values to, the "a", "b", and "c" absorption bands.

Approach

In this experiment the $HgBr_2$ will be placed into an evacuated (~10^{-6} torr) absorption cell made of Spectrasil tubing with Suprasil windows, both are a UV grade of fused quartz and products of Heraeus Amersil, and filled with about 250 torr of ultrapure helium. The absorption cell will be placed into a vacuum oven that was specifically designed for this

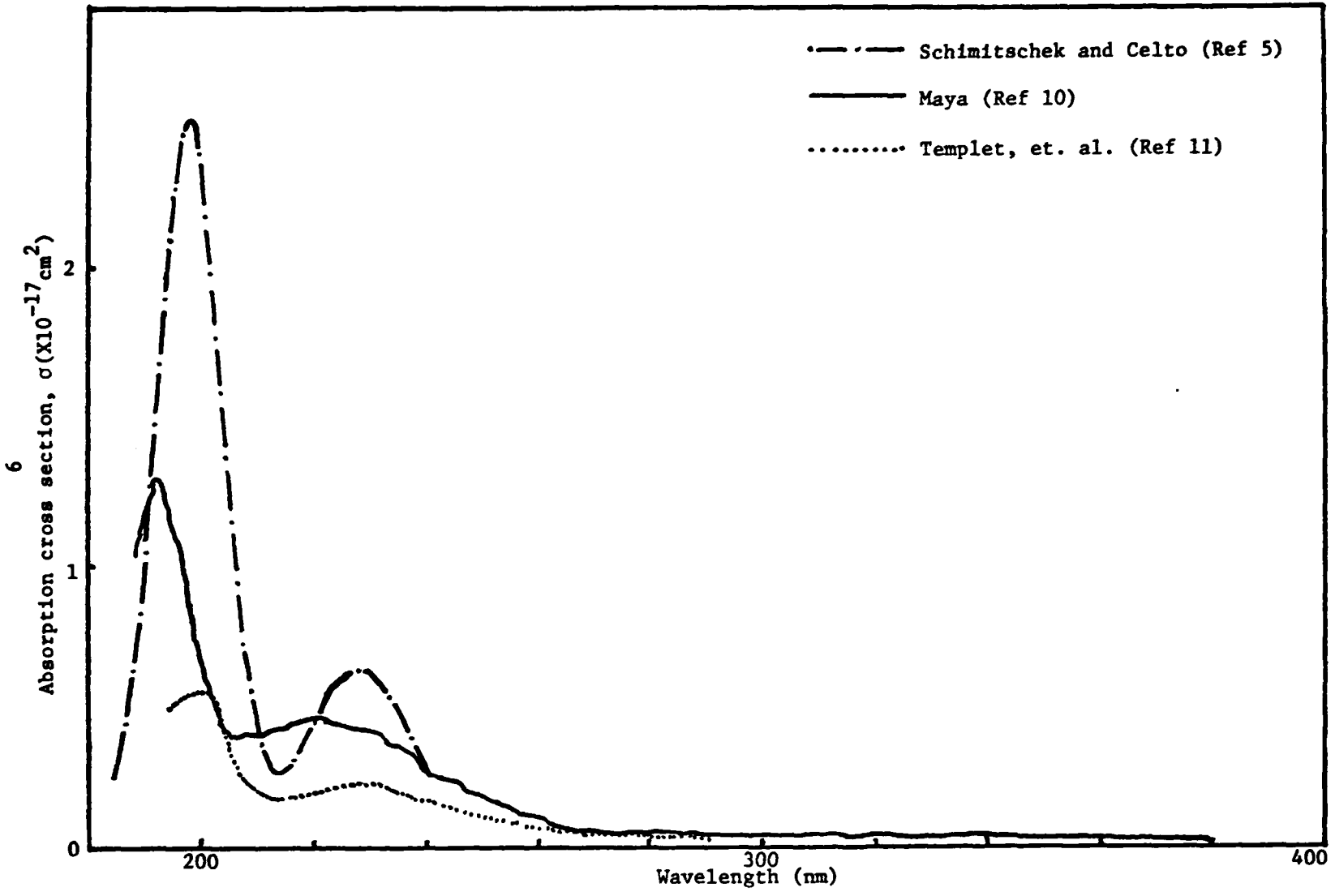

Figure 3: Comparative graph of available $HgBr_2$ cross section measurements.

experiment. See Appendix C for detailed diagrams of the oven components and the materials used for each.

Ultraviolet radiation from 175.0 nm to 325.0 nm emitted from a windowless capillary-type hydrogen discharge lamp ("Hinteregger" type) will be selected by a scanning monochromator with 50 μm entrance and exit slits, which will provide a 0.25 nm FWHM resolution. This UV radiation will be passed through the absorption cell at various temperatures, resulting in various vapor pressures of the $HgBr_2$, and then onto a sodium salicylate window. The resulting fluorescence of the sodium salicylate window will be detected by a photomultiplier with the output signal being amplified and stored, after analog-to-digital conversion, in a minicomputer. A copy of the information in the minicomputer can then be sent to a digital x-y plotter for graphic output or to a paper tape punch for permanent storage. This set-up will allow for continuous monitoring of the spectra as they are being produced.

The pressure of the monochromator will be maintained at about 10^{-6} torr as will the input and output cooling flanges on the absorption oven (specifics on the absorption oven will be explained in the next chapter). The body of the oven will be pumped to a pressure of about 10^{-2} torr and flushed with grade 6 helium (1 ppm contaminants at maximum) several times before any spectra are recorded. This is all necessary to insure the removal of possible contaminants in the system, such as H_2O, O_2, CO_2, or H_2.

The minicomputer will be programmed to average the input signal over a given time period, which will be set at 0.8 sec for this experiment. This averaging time, 0.8 sec, has been chosen to achieve good resolution with the shortest possible scan time. Since the region of interest is

from 175.0 nm to 325.0 nm (150.0 nm scan), it can be divided into 1125 intervals at a sweep rate of 10.0 nm/min at the chosen averaging time. These numbers should yield good resolution, since a plausible criterion is one where the sweep rate does not exceed the resolution of the monochromator divided by four or five RC-time constants. The time constant to be used for this experiment is 0.1 sec for all spectral scans. So the sweep rate showed should comply with the following equation:

$$S < R/(4 \text{ or } 5)\tau \qquad (7)$$

where

S = Sweep rate

R = Resolution of the monochromator

τ = Time constant

Choosing the 5, to be safe, it is found that the sweep rate must not exceed 30 nm/min. Therefore the monochromator will be set at 10 nm/min, this will lengthen the scan time some but will ensure good resolution.

II. Equipment

The equipment needed for this study was available, with the exception of the absorption oven and absorption cell which had to be made. The equipment used is as follows: (See block diagram Figure 4).

1. McPherson Vacuum Ultraviolet Scanning Monochromator #235
2. McPherson Photomultiplier (14-stage)
3. McPherson UV Source #630 ("Hinterreger"-type)
4. Superior Electric Co. Powerstat Type 116
5. Digitec Platinum Resistance Thermometer #551-4
6. Spellman High Voltage Source #HP5PH500SRX
7. Dymec Digital Volt Meter #2401C (used as a frequency meter)
8. General Motors Combustable Gas Detector #130
9. Hewlett Packard Harrison 6516A DC Power Supply
10. Hewlett Packard #2116C Minicomputer
11. Hewlett Packard #2644A Computer Terminal
12. Hewlett Packard #7610A Digital Plotter
13. Hewlett Packard #3480B Digital Volt Meter
14. Hewlett Packard #3484A Multifunction Unit
15. MKS Baratron Pressure Head Type 90
16. MKS Baratron Auto-Digital Pressure Meter Type 100A
17. MKS Temperature Control Unit Type 1090-1
18. Current-to-Voltage (I/V) Converter (Gains: 10^4-10^{12} volts/amp)
19. Current Regulator (Constructed by SRL, 0.5% accuracy)
20. Absorption oven (Built to specifications, details in next section)
21. Absorption cell (Built to specifications, See Figure 5)

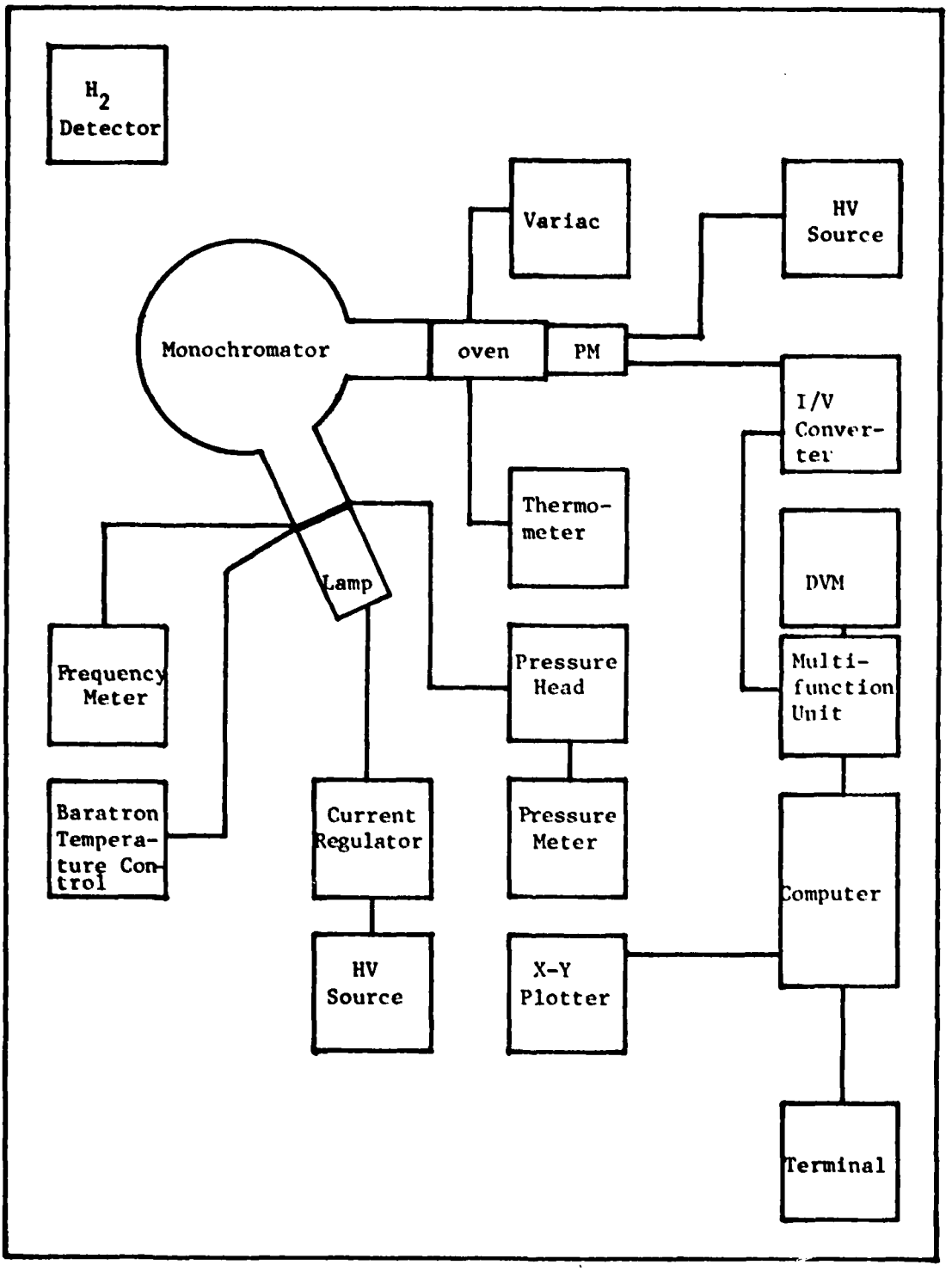

Figure 4: Block Diagram of Apparatus

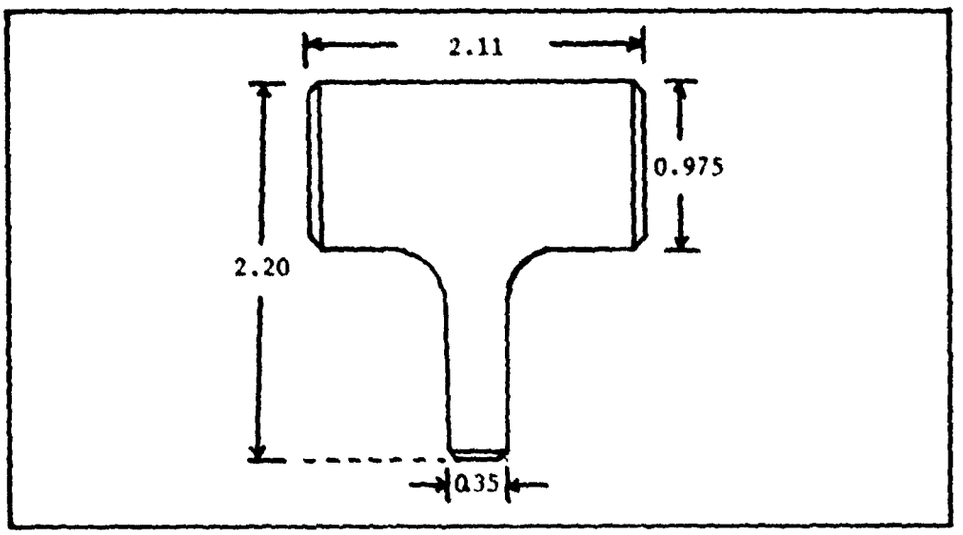

Figure 5: Cross-section View of the Absorption Cell

Absorption Oven

The absorption oven, which had to be built to specifications (see Figures 6 and 7 and Appendix C), was an important part of this study. It was necessary to choose material for their thermal properties as well as their machining and welding properties. The entire oven had to be vacuum leak tight, about 10^{-6} torr, and had to achieve a uniform temperature profile. The oven will be explained in three parts, the first is the input and output cooling flanges, the second is the oven body, and the third is the cold-finger temperature sensor. These three parts are identified in Figure 7.

The input and output cooling flanges were each made of two circular plates, 5 in. diameter and 0.25 in. thick, that were connected with a hollow tube 2.0 in. o.d., 1.94 in. i.d., and 1.0 in. long. All materials in the cooling flange were #304 Stainless Steel, chosen for its low thermal conducting properties, high strength, and good vacuum qualities. The cooling flanges were important; their function was to protect the monochromator on the input side, and reduce the thermal generation of noise in the photomultiplier on the output side. A single wrap of ¼ in. copper tubing was placed around the stainless steel tubing and against the first and last plate (the ones that connected the oven to the monochromator and the photomultiplier). These were used as water cooling lines to further aid the function of the cooling flanges. With an external temperature, at the oven body, of 200°C the first and last flanges remained at or slightly below room temperature.

The oven body was constructed entirely of #6061 aluminum and consisted of one input plate with a 5.0 in. diameter and ½ in. thickness (this plate housed the input window which was a Suprasil fused quartz window), and two

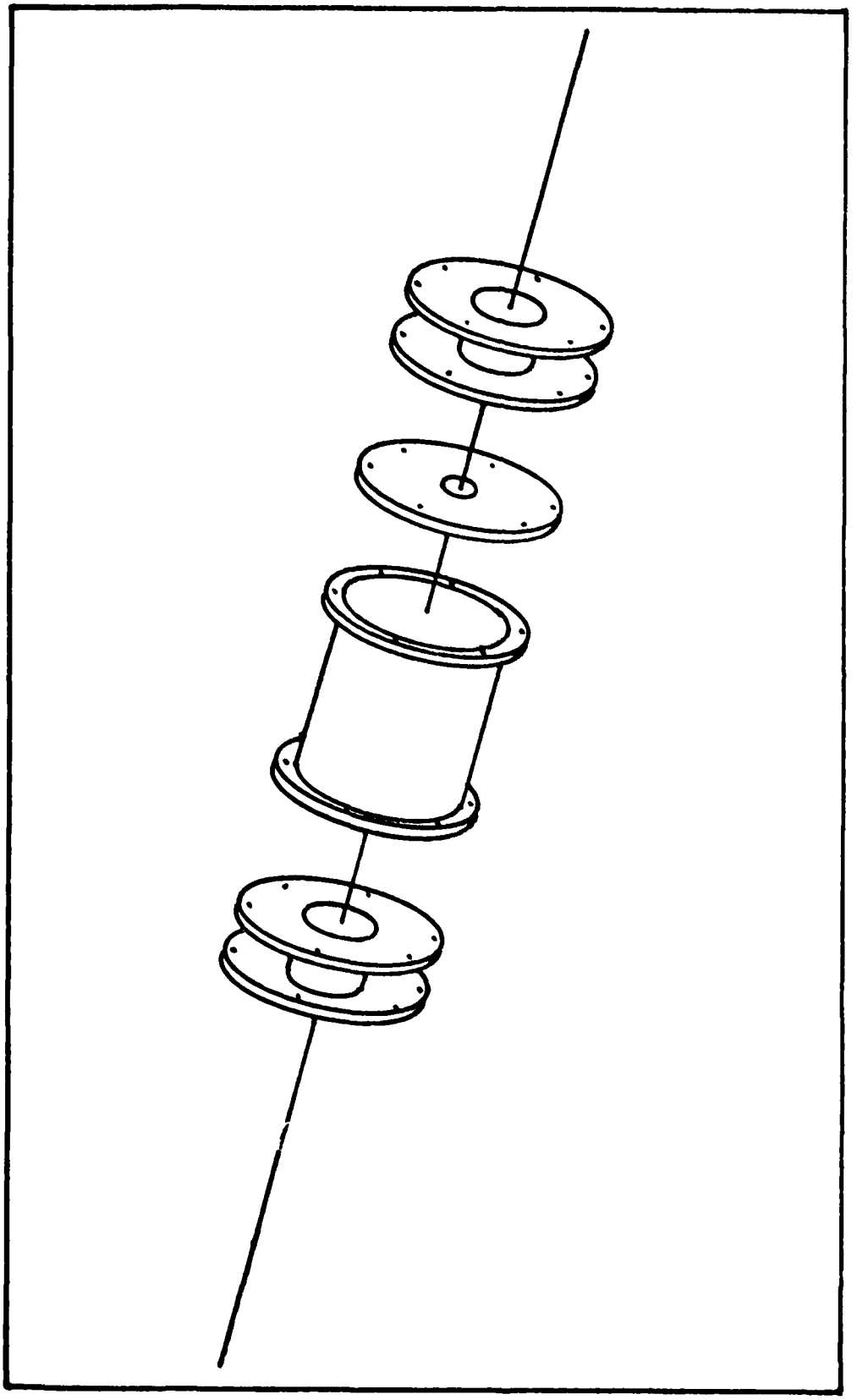

Figure 6: Exploded View of the Oven

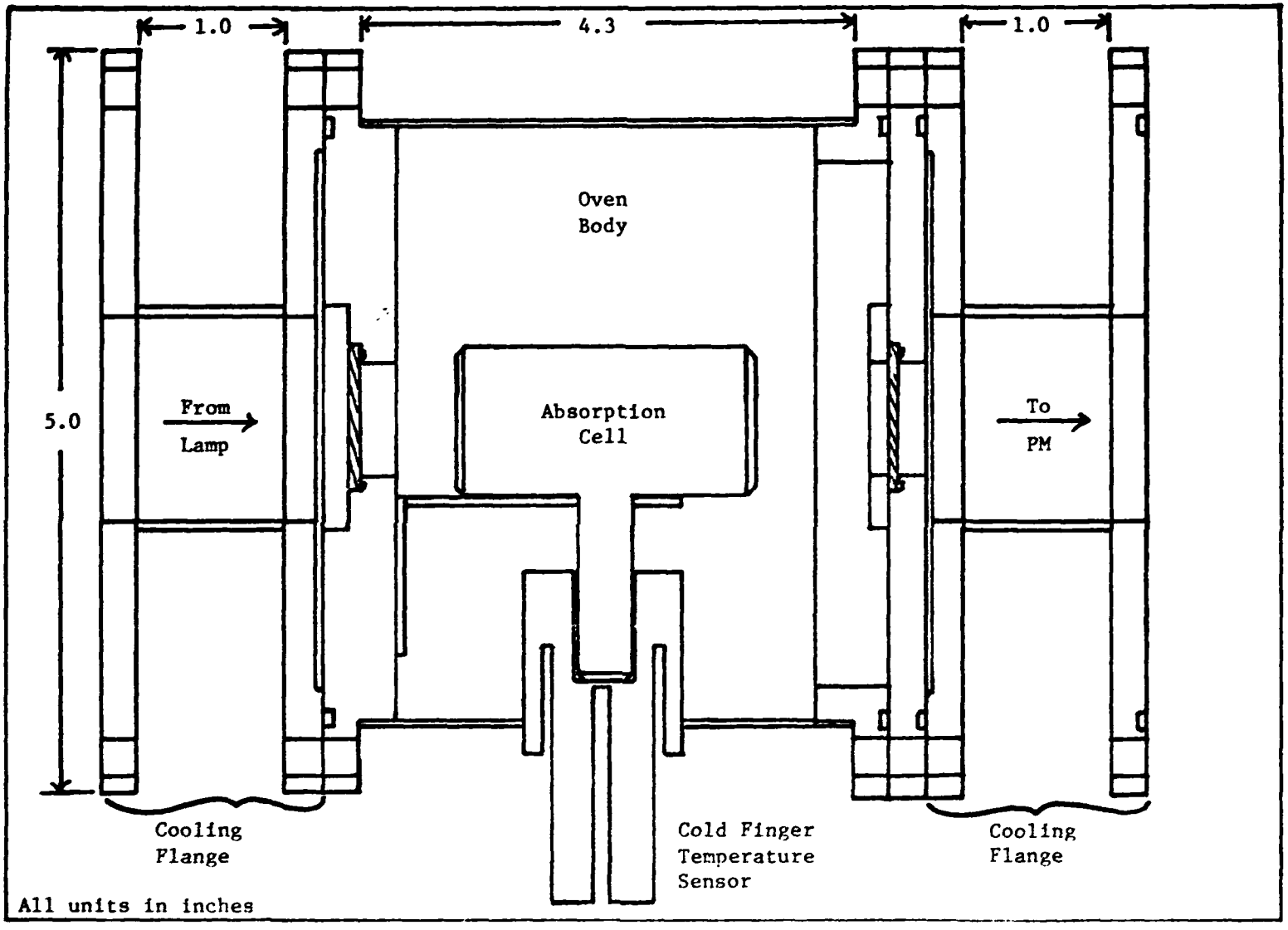
1.0
4.3
1.0
Oven
Body
5.0
From
Lamp
Absorption
Cell
To
PM
Cooling
Flange
Cold Finger
Temperature
Sensor
Cooling
Flange
All units in inches

output plates both with a 5 in. diameter. The first output plate was ½ in. thick and had a 3½ in. hole cut thru it in the middle. This allowed access to the internal portion of the oven to remove or replace the absorption cell. The second output plate was ¼ in. thick and housed the output window which was the same type as the input window. The second output plate was the only part of the absorption oven that was available and, therefore, did not need to be constructed. The oven wall, which connected the input and output plates, was cylindrical, 4.3 in. long, with a 4.0 in. i.d. and a 0.060 in. wall thickness. It was necessary to mill the input plate, the oven wall and the first output plate from one solid piece of aluminum to ensure a vacuum seal.

The cold-finger temperature sensor plug was made of #6061 aluminum also. This solid plug had two holes drilled in it, one from the top to house the cold-finger of the absorption cell, and the other from the bottom to house the platinum resistance thermometer. A metal spacing of these two holes was necessary to ensure vacuum , but it was less than 0.060 in. An air annulus was cut into the plug to isolate the contact point of the temperature sensor and the cold-finger from the oven wall, and the hot gasses at the oven wall. The annulus was open to ambient room air, but could have been further cooled by forced air, if it was necessary. The plug was not heated and, due to the air annulus, was isolated from the wall heat. Therefore, the temperature measured at the cold-finger will represent the coldest point in the absorption cell, which in turn will be responsible for determining the vapor pressure of the $HgBr_2$. With an external temperature, at the oven wall, of 200°C, the cold-finger temperature sensor indicated 175°C.

The oven body was heated by externally wrapped electrical heating tape, which did not touch the cooling flanges or the temperature sensor plug. Two small aluminum tubes, 1/8 in. o.d. and 1/16 in. i.d., were used to introduce helium into the oven body. The input and output helium tubes were both wrapped twice around the outside of the oven wall under the heating tape. This allowed the helium to be heated before it was introduced in the oven, and allow it to remain hot until it was well away from the oven body.

III. Experimental Procedure

The wavelength range of interest extended from 175 nm to 325 nm. The lower boundary was set by the transmission characteristics of the fused quartz windows used in the oven and on the absorption cell; the upper boundary was chosen to ensure coverage of the first three absorption bands of the $HgBr_2$.

The hydrogen flow to the Hinteregger type discharge lamp was set at about 10 sccm, enough to maintain a pressure of 1.000 ± .002 torr at the discharge. The current through the discharge was set at 100 mA with less than 0.5% fluctuation, this resulted in a voltage drop across the discharge of about 1 Kv. Water flow to the lamp, for cooling, was monitored by a DVM, used as frequency meter, that was connected to a rotating pinwheel in the input line. It was noted that if the fluctuations in the rotations of the pinwheel, or fluctuations in the water flow, exceeded $\pm 5\ sec^{-1}$, the intensity of the lamp would drift due to the changes in the operating temperature. This experiment did not require maximization of lamp intensity as a function of operating temperature, but only to choose a water flow, and hence an intensity, that was consistent and repeatable.

The 50 μm wide entrance and exit slits on the monochromator provided a 0.25 nm and FWHM resolution. The grating used has a blaze angle of 3°35", blazed for 150.0 nm, and a grating constant of 600 mm^{-1}. The sweep rate for the monochromator was set at 10.0 nm/min to yield good resolution for the chosen time constant (see page 11 for details). The I/V converter on the output was set for a gain of 10^6 volts/amp with a 0.1 μF capacitor for most scans, and a gain of 10^7 volts/amp with a 0.01 μF capacitor for the transmission scans at higher temperatures, since the amplification

III. Experimental Procedure

The wavelength range of interest extended from 175 nm to 325 nm. The lower boundary was set by the transmission characteristics of the fused quartz windows used in the oven and on the absorption cell; the upper boundary was chosen to ensure coverage of the first three absorption bands of the $HgBr_2$.

The hydrogen flow to the Hinteregger type discharge lamp was set at about 10 sccm, enough to maintain a pressure of 1.000 ± .002 torr at the discharge. The current through the discharge was set at 100 mA with less than 0.5% fluctuation, this resulted in a voltage drop across the discharge of about 1 Kv. Water flow to the lamp, for cooling, was monitored by a DVM, used as frequency meter, that was connected to a rotating pinwheel in the input line. It was noted that if the fluctuations in the rotations of the pinwheel, or fluctuations in the water flow, exceeded $\pm 5\ sec^{-1}$, the intensity of the lamp would drift due to the changes in the operating temperature. This experiment did not require maximization of lamp intensity as a function of operating temperature, but only to choose a water flow, and hence an intensity, that was consistent and repeatable.

The 50 μm wide entrance and exit slits on the monochromator provided a 0.25 nm and FWHM resolution. The grating used has a blaze angle of 3 35", blazed for 150.0 nm, and a grating constant of 600 mm^{-1}. The sweep rate for the monochromator was set at 10.0 nm/min to yield good resolution for the chosen time constant (see page 11 for details). The I/V converter on the output was set for a gain of 10^6 volts/amp with a 0.1 μF capacitor for most scans, and a gain of 10^7 volts/amp with a 0.01 μF capacitor for the transmission scans at higher temperatures, since the amplification

was needed. These settings yielded a 0.1 sec time constant for all of the scans.

The signal from the I/V converter was sent to a DVM and finally stored in a minicomputer. A copy of the data could then be sent to an x-y plotter for a graphic output or to a paper tape punch for permanent storage for future use.

When the system was first assembled, the empty absorption oven was pumped to the 10^{-6} torr range and baked out for eight hours on each of three consecutive days. After the bake-out was completed, the lamp was turned on and several spectral scans were made, with the oven empty, while the oven was heated from room temperature to temperatures in excess of 200°C. The output showed no change in the transmitted light as a function of oven temperature.

The empty absorption cell, after being cleaned, was placed into the oven and several spectral scans were made at various temperatures, from 25°C to 200°C external, and there were no changes in the output data. This output data represented the incident radiation to be used in computing the absorption cross section. See Figure 8 for a graph of the spectrum used as the incident radiation. This figure, like all of the transmission spectra, has a relative intensity scale on the vertical axis, which was set to obtain a maximum deflection for the peak of the curve.

The absorption cell was then removed, cleaned, pumped to a pressure of 10^{-6} torr, filled with 4.5 mg of $HgBr_2$ crystals and 253.0 torr of ultra-pure helium (at room temperature) to aid in the quenching reaction, and returned to the absorption oven for the transmission scans.

The absorption measurements were taken at 110°C, 119.9°C, 128°C, 129°C and 151°C with a fluctuation of ±0.2°C during the scans as monitored

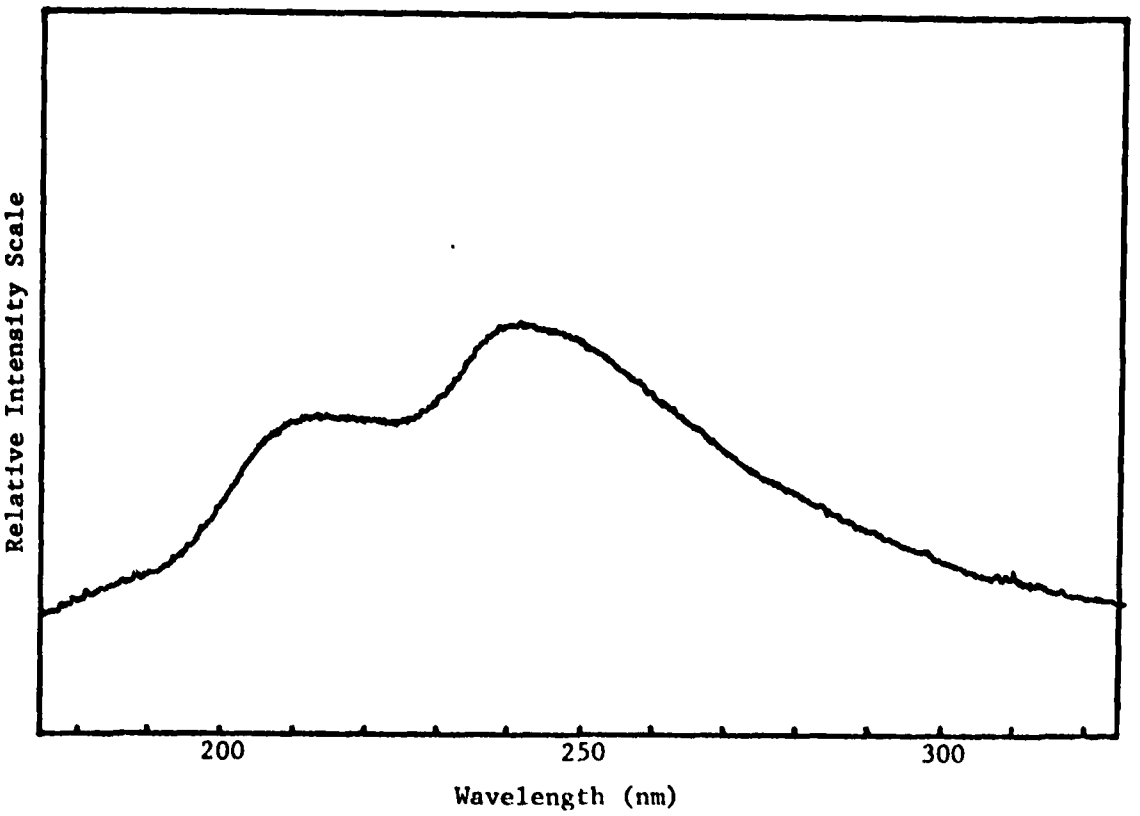

Figure 8: Spectrum of Probing Radiation.

by a platinum resistance thermometer at the cold-finger temperature sensor. These temperatures produced vapor pressures, in torr, of the $HgBr_2$ of 0.20, 0.38, 0.62, 0.66, and 2.77 respectively. The temperature fluxtuations would yield a maximum error in the pressure of about ±1%. See Figure 9 for a typical transmission curve. All of the transmission curves are assembled in Appendix A.

Higher temperatures, and hence higher pressures, were attempted, but at these high number densities the input radiation was extinguished over a fairly large range, and in these ranges the only radiation to reach the photomultiplier was that due to fluorescence of the HgBr which was a very small amount. See Appendix B for a computation on the fluorescent noise.

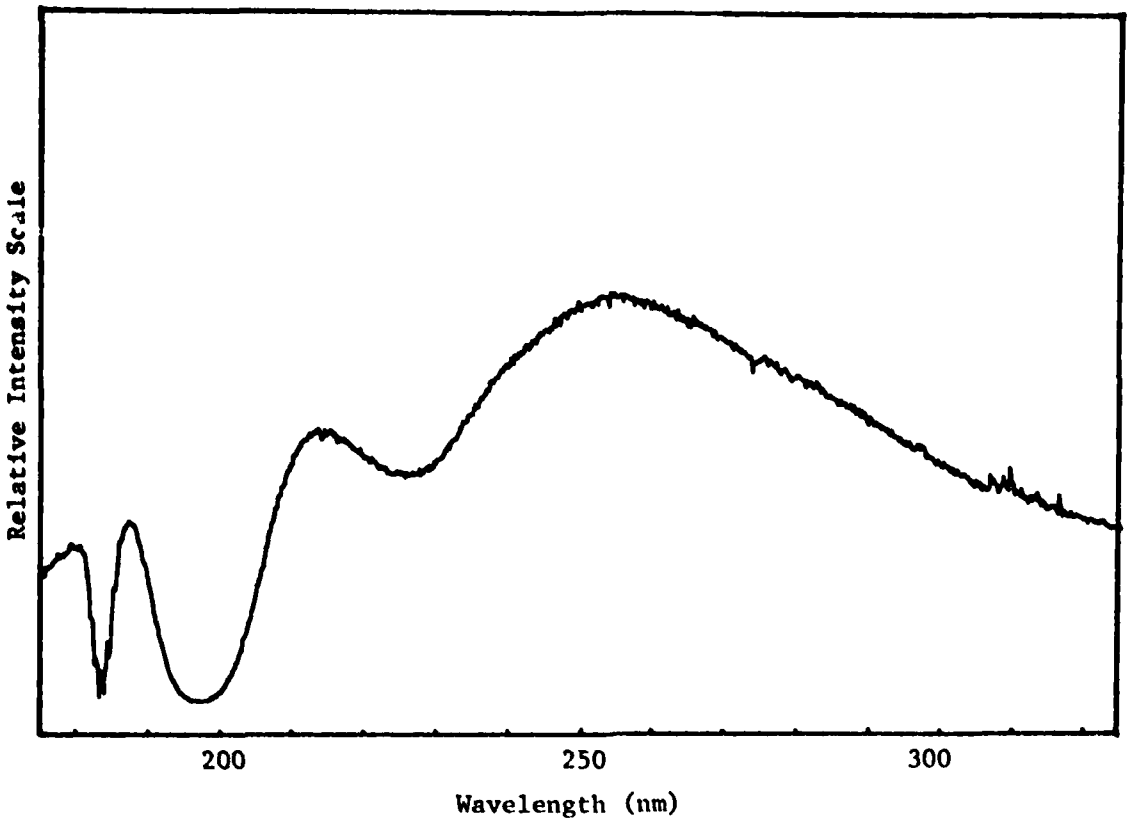

Figure 9: Transmission Curve at 128°C

For an example of the extinguishing of the input radiation, and its effect on the measured cross section, see Figures 10 and 11 in the wavelength range of 193 nm to 204 nm.

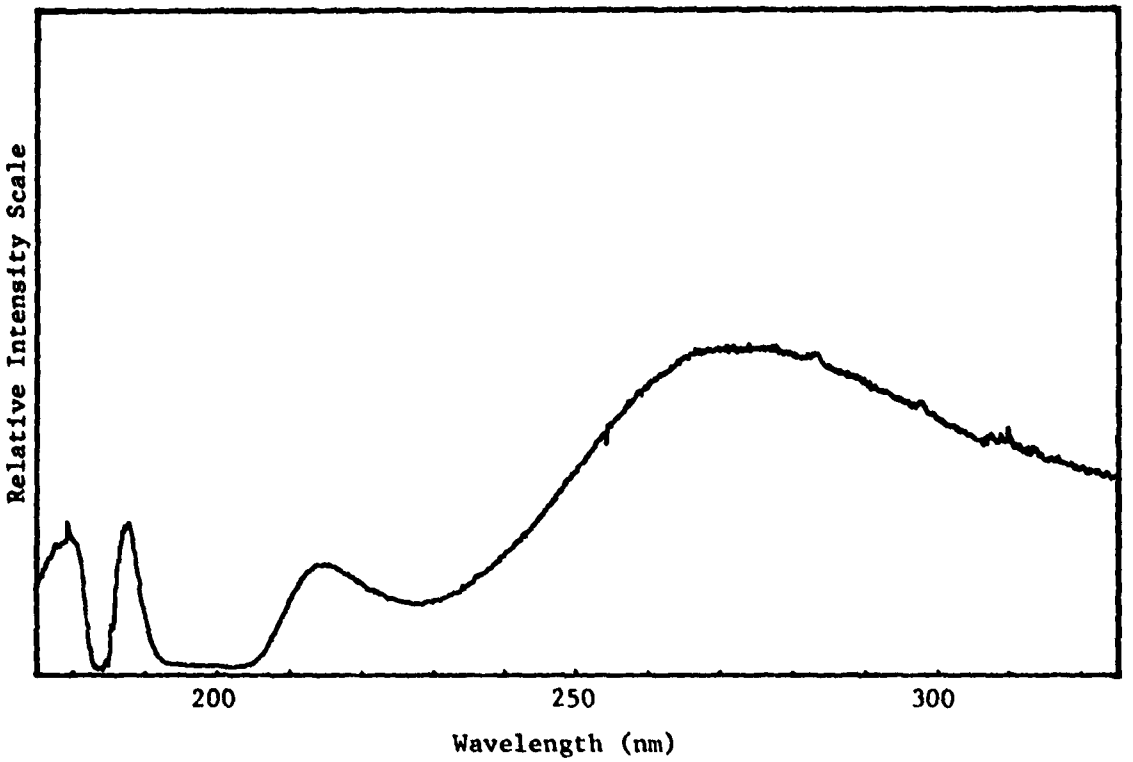

Figure 10: Transmission Curve at 151°C

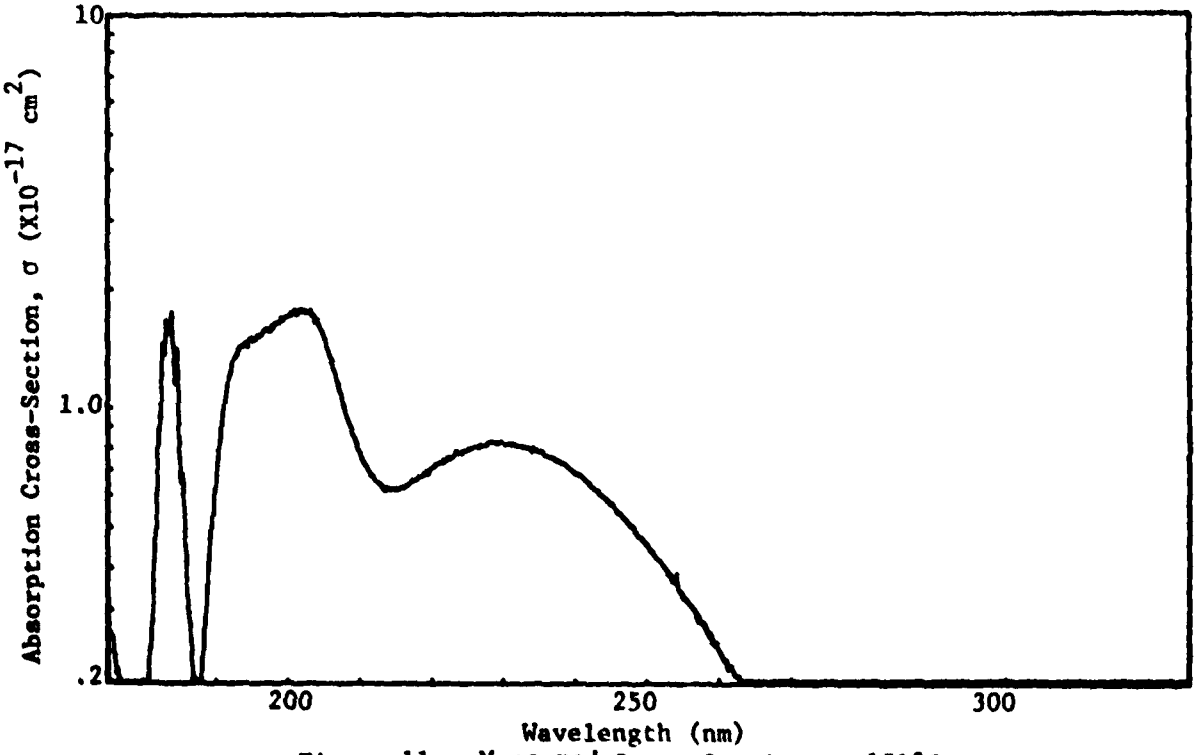

Figure 11: Measured Cross Section at 151°C

IV. Results and Discussion

The graphic results of this experiment can be seen in Appendix A. The computed cross section of $HgBr_2$ for the scans at 1.0°C, 119.9°C, 128°C, and 129°C, all ±0.2°C, show very good, consistent information. The absorption cross section computed for the scan at 151°C (2.27 torr of $HgBr_2$) indicated a change in the "b" absorption band. This change has been accredited to an excessive amount of absorbers extinguishing the input radiation, which in turn would cause the cross section curve to flatten and spread.

The absorption cross section was computed, by a minicomputer, as a function of wavelength using the Beer-Lambert Law:

$$\frac{I_o(\lambda)}{I(\lambda)} = \exp[n\sigma(\lambda)L] \tag{8}$$

where

$I_o(\lambda)$ = Incident radiation at λ

$I(\lambda)$ = Transmitted radiation at λ

n = Number density of $HgBr_2$

L = Path length through the absorbing media

$\sigma(\lambda)$ = Absorption cross section at λ

The number density of $HgBr_2$ was computed by making a pressure and temperature correction to Loschmidt's number ($2.69 \times 10^{19} cm^{-3}$). But the pressure was also computed as a function of temperature. This leads to a number density equation of

$$n = \frac{2.69 \times 10^{19}}{760}\left[10^{(-0.2185\ A/T_1 + B)}\right]\left(\frac{273}{T_2}\right) \tag{9}$$

where

A = 19072.7

B = 10.18100

T_1 = Temperature (°K) used to compute vapor pressure of $HgBr_2$

T_2 = Temperature (°K) used to compute number density of $HgBr_2$

In this equation T_1 does not necessarily equal T_2. T_1 is used to determine the vapor pressure of $HgBr_2$ and should be the coldest temperature in the absorption cell. This is the reason for the cold-finger, since the temperature measured there should be T_1. On the other hand, T_2 determines the number density and it should be a localize temperature. The system was allowed to reach thermal equilibrium before absorption measurements were taken, therefore the entire absorption region of the cell would have reached a constant temperature that was greater than T_1 but less than or equal to the oven wall temperature. For the computation of the absorption cross section, the temperature recorded at the cold-finger was used to compute the pressure and the number density. This introduced an error in the final computation of no more than 5.0% at 150°C and an even smaller error for lower temperatures. This leads to a final equation for the cross section of

$$\sigma(\lambda) = \frac{760}{2.69 \times 10^{19}} \left(\frac{T}{273}\right) \left[10^{(0.2185\ A/T\ -\ B)}\right] \ln\left(\frac{I_o(\lambda)}{I(\lambda)}\right) \qquad (10)$$

$I_o(\lambda)$ and $I(\lambda)$ as well as T and L, were entered into the computer during a scan and the cross section was computed, by the computer; and output was obtained graphically on an x-y plotter. See Appendix D for the controlling computer program.

A quick analysis shows agreement with this previous published data (see Figure 3) on the location of the peaks of the "a" and "b" bands at about 230 nm and 200 nm respectively, but again differs with the magnitudes. The values measured here place the peak of the "b" bands at $\sim 3.4 \times 10^{-17} cm^2$ which is about 1.3 times greater than the value reported by Schimitschek and Celto (Ref 5), and 2.7 and 8 times greater than the values reported by Maya (Ref 8) and Templet, et. al. (Ref 9), respectively. The value of the peak of the "a" band for this report is $\sim 9.8 \times 10^{-18} cm^2$ which is about 1.6 times greater than the value reported by Schimitschek and Celto, 2.5 times greater than the value reported by Maya, and 5 times greater than the value reported by Templet, et. al. And, finally, this report does include the "c" absorption band at ~183.6 nm and can be seen in Figure 12. The fine structure that appears on the peak of the "c" band is due to vibrational transitions that occur in the $HgBr_2$ when radiated with light in the wavelength range of 182.6 nm to 185.4 nm. These transitions have been studied spectroscopically, with much higher resolution, on several occasions; one such study was reported by Gedanken, et. al. (Ref 7) in 1969.

This clearly shows that there is a great deal of difference in the available information, not only in past work but also when compared to this study. However, the information presented here is considered to be the most accurate to date for three reasons:

(1) Two of the previous published studies reported the cross section starting at about 185 nm. At this point they should have recorded absorption by the "c" band, but they did not. This could be due to the transmission characteristics of the optics used, and, if so, it is not known what correction would be needed for the 200-230 nm range. The optics

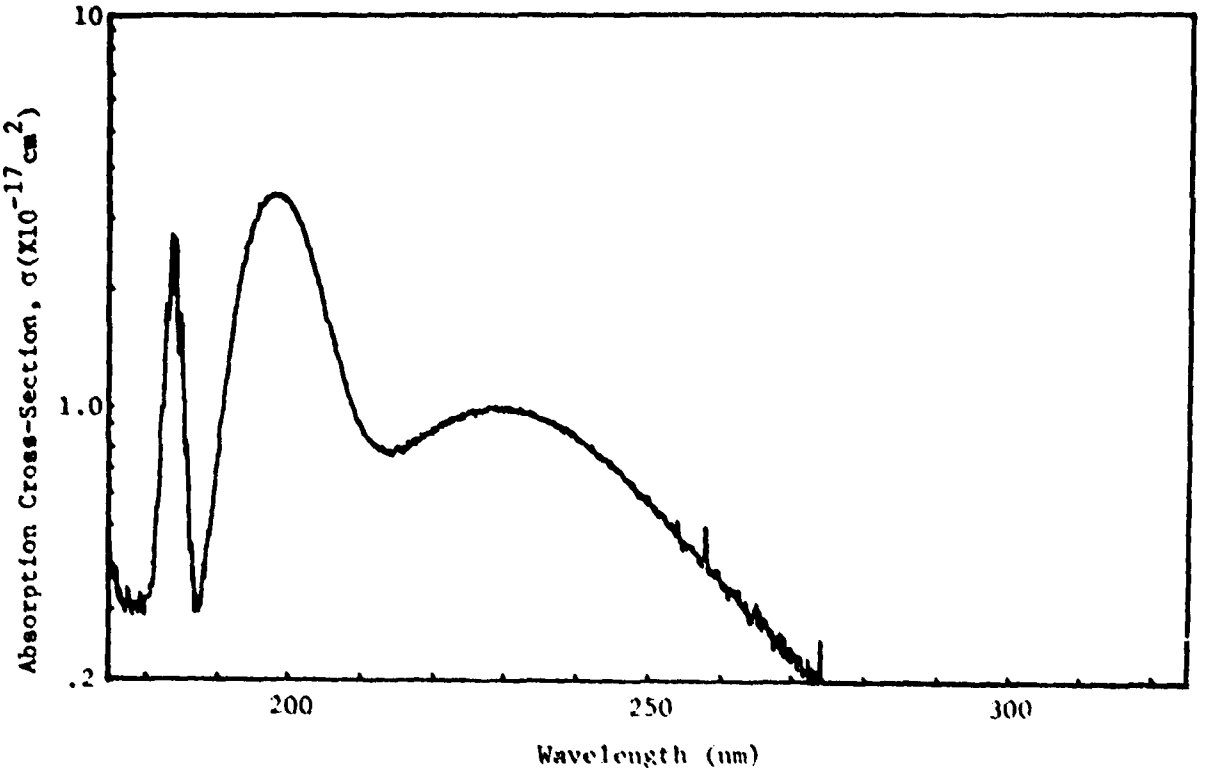

Figure 12: Measured Cross Section at 129°C

used for this experiment had fairly constant high transmission over the entire wavelength range of 175-325 nm.

(2) Only one of the three previous reports had any information pertaining to experimental procedure and apparatus used; and, in it the author used a polychromatic source. Although the effects of a polychromatic source were considered; it still could have introduced problems. If the photon flux from the lamp used was significantly high (on the order of the number density) then the absorption-dissociation reactions could have lowered the number density of $HgBr_2$ molecules for the entire spectral scan. This in turn would have yielded a measured cross section with the magnitude of the peaks smaller than the true values.

(3) Finally, two of the reports made no mention of possible errors introduced by the experimental system, nor could these errors be deduced. For the experiment reported in this paper, the greatest sources of error were in the temperature measurement accuracy and in the resolution of the monochromator. The error in the temperature measurements was estimated to introduce about 10-15% error in the cross section; and the error due to the resolution would only effect the "c" absorption band where there was fine structure. Here the error would tend to reduce the actual cross section but not by a significant amount. Finally, overall system error was estimated to be no more than 20%. The one previous study that did report an estimated error agrees with the present work, when errors are considered, on the magnitude of the "b" band, but still differs with the magnitude of the "a" band by a factor of 1.7.

Analyzing the cross section curve yields some interesting information. It is known that exciting an $HgBr_2$ molecule into the "a" state or "b" state will cause the molecule to dissociate since these are dissociative, or unbound, states. Both states will yield an HgBr molecule; the HgBr from the "a" state of the $HgBr_2$ will be in the "X" state and the HgBr from the "b" state of the $HgBr_2$ will be in the "B" state (see Figure 2). As of yet nobody has reported transitions to or from the "A", or first excited, state of HgBr. The lasing that has been observed operated on the HgBr ($B \rightarrow X$) transition.

The "c" band differs slightly from the "a" and "b" bands. Although it is an absorption continuum which implies it is a dissociative state, it has some vibrational fine structure which implies it is a bound state. Putting these two facts together, along with the fact that no further fine structure is present that was lost due to restriction in the

resolution (see Gedanken, et. al. (Ref 7) for a spectrum of this region with a much higher resolution), one arrives at the conclusion that the "c" state for $HgBr_2$ is a predissociative state, or a bound state that is overlapped by a higher level dissociative state. Many of the $HgBr_2$ molecules that are excited into the "c" state will make a radiationless transver to the overlapping dissociative state and dissociate. The time for the transfer is shorter than the time of rotation, but longer than the time of vibration. Hence, rotational fine structure is lost, some vibrational fine structure is preserved, and the absorption band remains a continuum as it would for any dissociative state. When an $HgBr_2$ molecule dissociates from the "c" state it is not known what state the resulting HgBr molecule will be in, a good guess would be the "C" state. Furthermore, it is not known what effect this molecule would have on the HgBr laser. If the resulting HgBr from the $HgBr_2$ excited into the "c" state would make a transition from a higher energy state to the "B" state, then it could possibly enhance the laser action. However, if it makes a direct transition to the ground state it could detract from the laser action since it could be populating the lower laser level.

Final analysis shows that if a photolytic pumped $HgBr_2$ laser is to be made, the pump chosen should deliver most of its energy in the 190-210 nm range since this would produce HgBr molecules in the "B" state. The pump used should not, however, deliver a significant amount of energy in the 215-250 nm range, since this would produce HgBr molecules in the "X" state and would tend to populate the lower laser level. This laser could only be produced with a fairly low vapor pressure of $HgBr_2$ or the pump intensity would not reach the molecules that are in the center of the

tube, for coaxial geometry, and the resulting laser beam would be an annulus instead of a smooth Gaussian profile.

V. Suggestions and Recommendations

It was stated that the largest source of error in this experiment was the uncertainty in the temperature measurements. It would be an improvement if a new method of measuring both the coldest temperature and the average equilibrium temperature for the absorption cell could be devised.

It was also stated that at the present time it is not known which excited state is populated by the HgBr molecule that is formed by a dissociated $HgBr_2$ molecule from the "c" state. Nor is it known if it will enhance or detract from the laser action operating on the HgBr ($B \rightarrow X$) transition.

Finally it would be interesting to see if the HgBr ($C \rightarrow X$) or HgBr ($D \rightarrow X$) transition, whichever upper state is formed by the dissociated $HgBr_2$ molecule from "c" state, would support laser action. The reasoning here is simple. A laser operating on this transition should have approximately the same optimum efficiency as a laser operating on the $B \rightarrow X$ transition but would have a much shorter wavelength (on the order of 300-350 nm, depending on the upper and lower vibrational levels).

References

1. J.H. Parks. Appl. Phys. Lett., 31: 192 (1977).

2. J.H. Parks. Appl. Phys. Lett., 31: 297 (1977).

3. J. Gary Eden. Appl. Phys. Lett., 31: 448 (1977).

4. E.J. Schimitschek, J.E. Celto, and J.A. Trias. Appl. Phys. Lett., 31: 608 (1977).

5. E.J. Schimitschek and J.E. Celto. Optics Lett., 2: 64 (1978).

6. Robert C. Weast (ed). CRC Handbook of Chemistry and Physics, 52 ed. (Chemical Rubber Company, Cleveland, 1971), P. D-171.

7. A. Gedanken, et. al. J. Mole. Spec., 32: 287 (1969).

8. K. Wieland. Z. Electrochem., 64: 761 (1960).

9. Jabob Maya. IEEE J. Quantum Ele., 15: 580 (1979).

10. Jabob Maya. J. Chem. Phys., 67: 4976 (1977).

11. P. Templet, et. al. J. Chem. Phys., 56: 5746 (1972).

12. Dennis F. Grosjean. Personal Communications.

APPENDIX A

Graphs

This comprises the incident radiation spectrum, the transmission curves, and the measured absorption curves for 110°C, 119.9°C, 128°C, 129°C, and 151°C. Each graph is presented on a full page to better represent the structure of the absorption (transmission) or absorption cross-section. The curves are recorded by temperature which inturn represents different pressures of the $HgBr_2$. The pressure of $HgBr_2$ as a function of temperature is given by Equation 1 and is graphically displayed in Figure 1 (page 6).

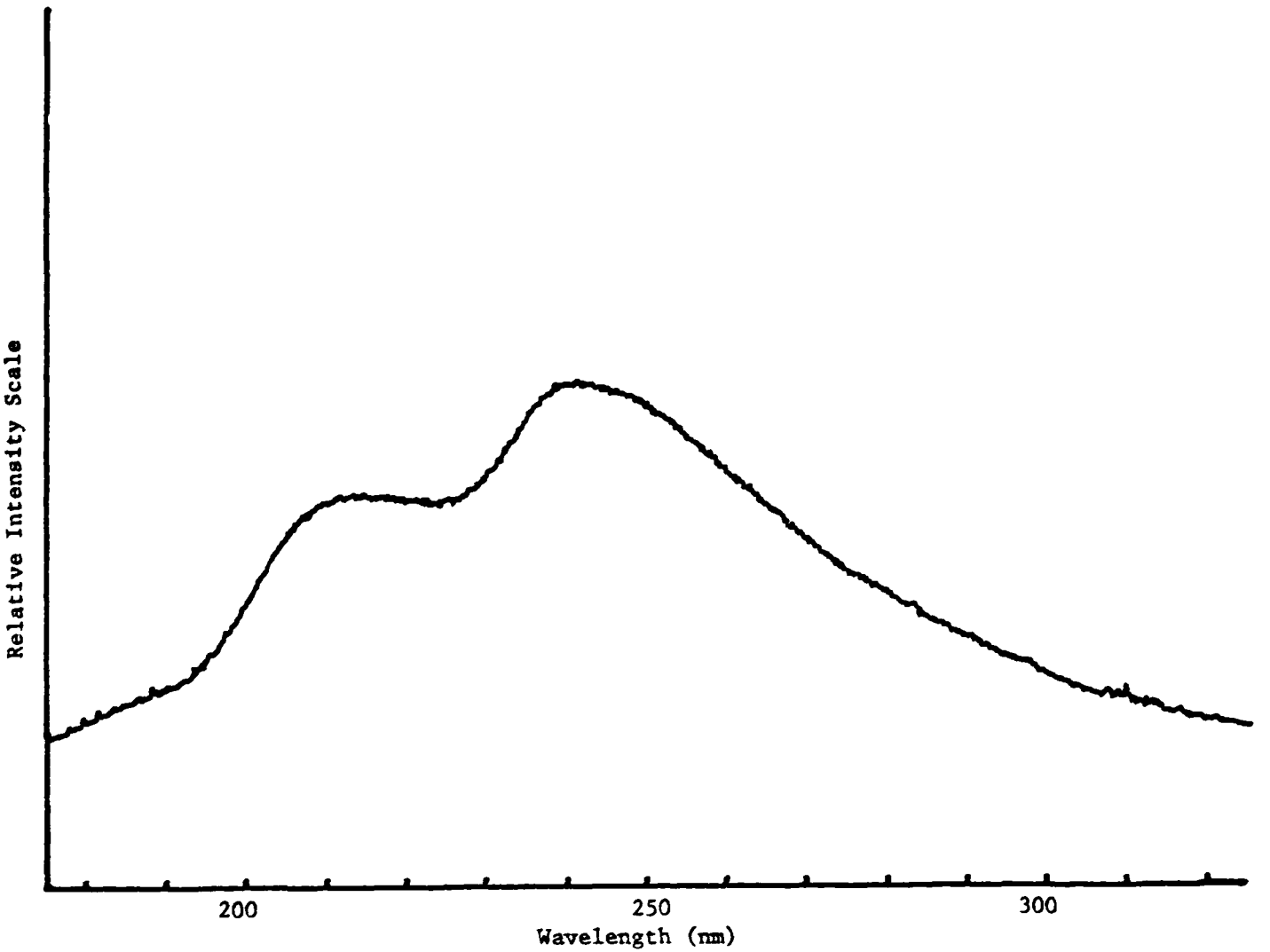

Figure 13: Spectrum of Probing Radiation

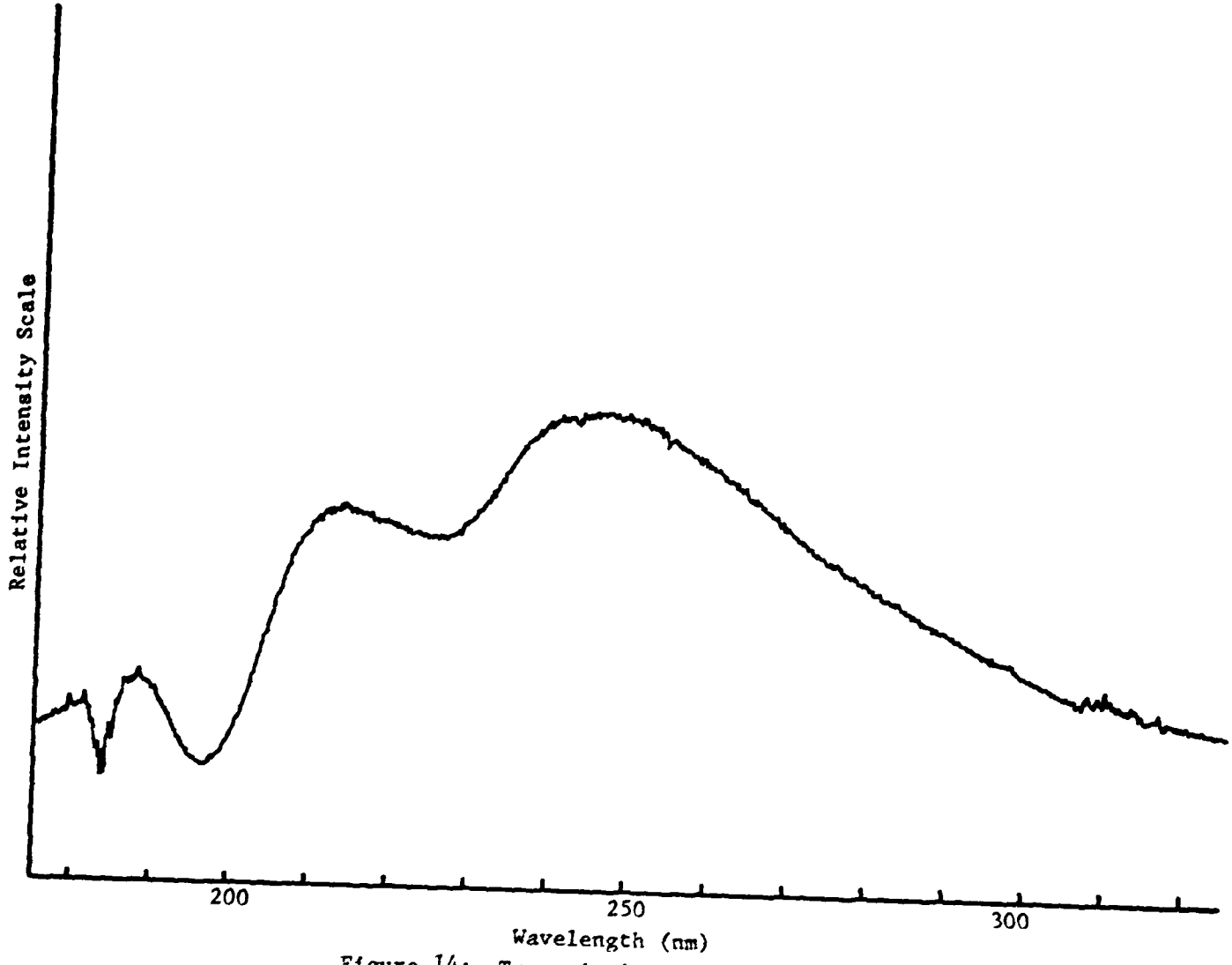

Figure 14: Transmission Spectrum at 110°C

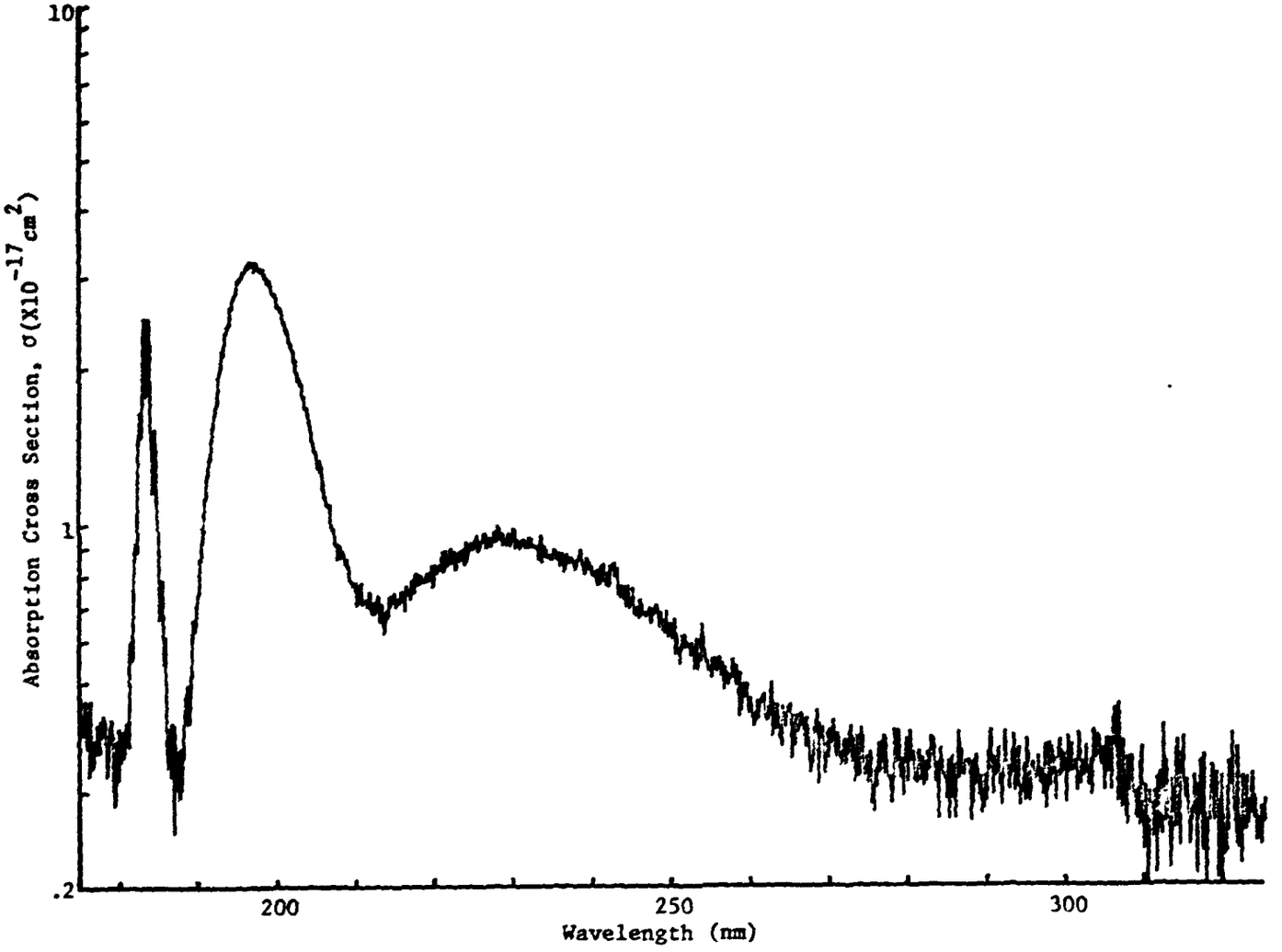

Figure 15: Measured Absorption Cross Section Curve at 110°C

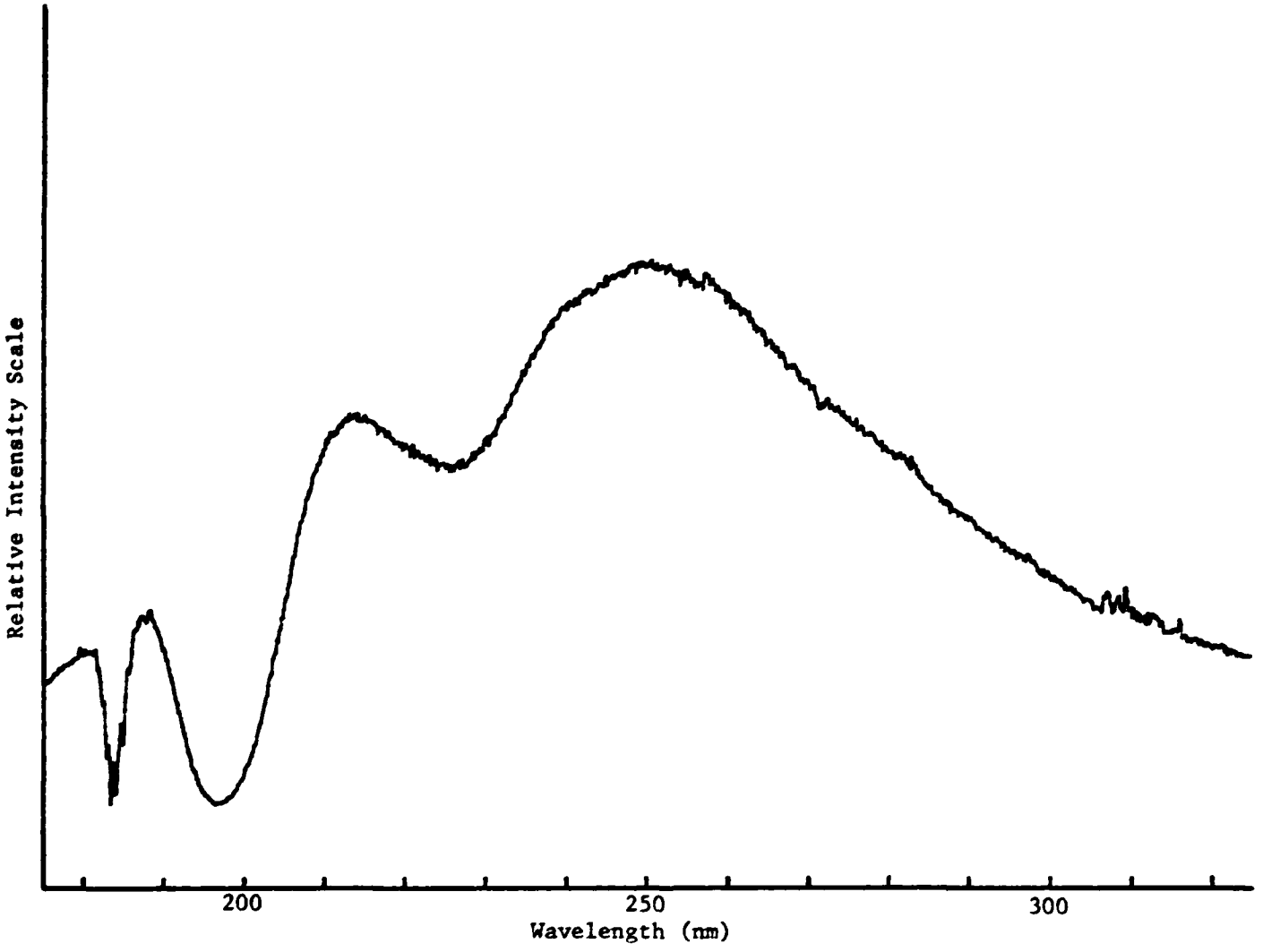

Figure 16: Transmission Spectrum at 119.9°C

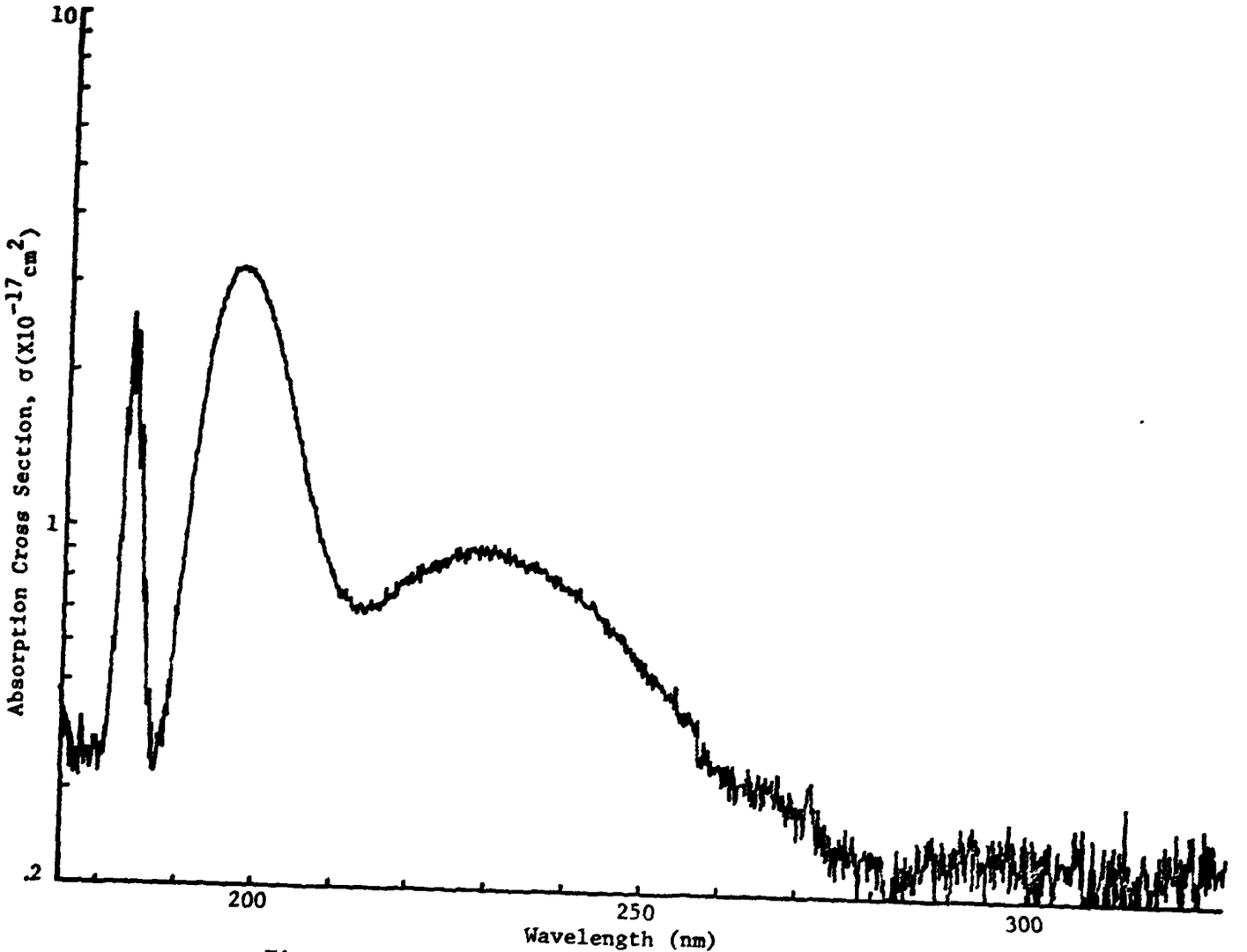

Figure 17: Measured Absorption Cross Section at 119.9°C

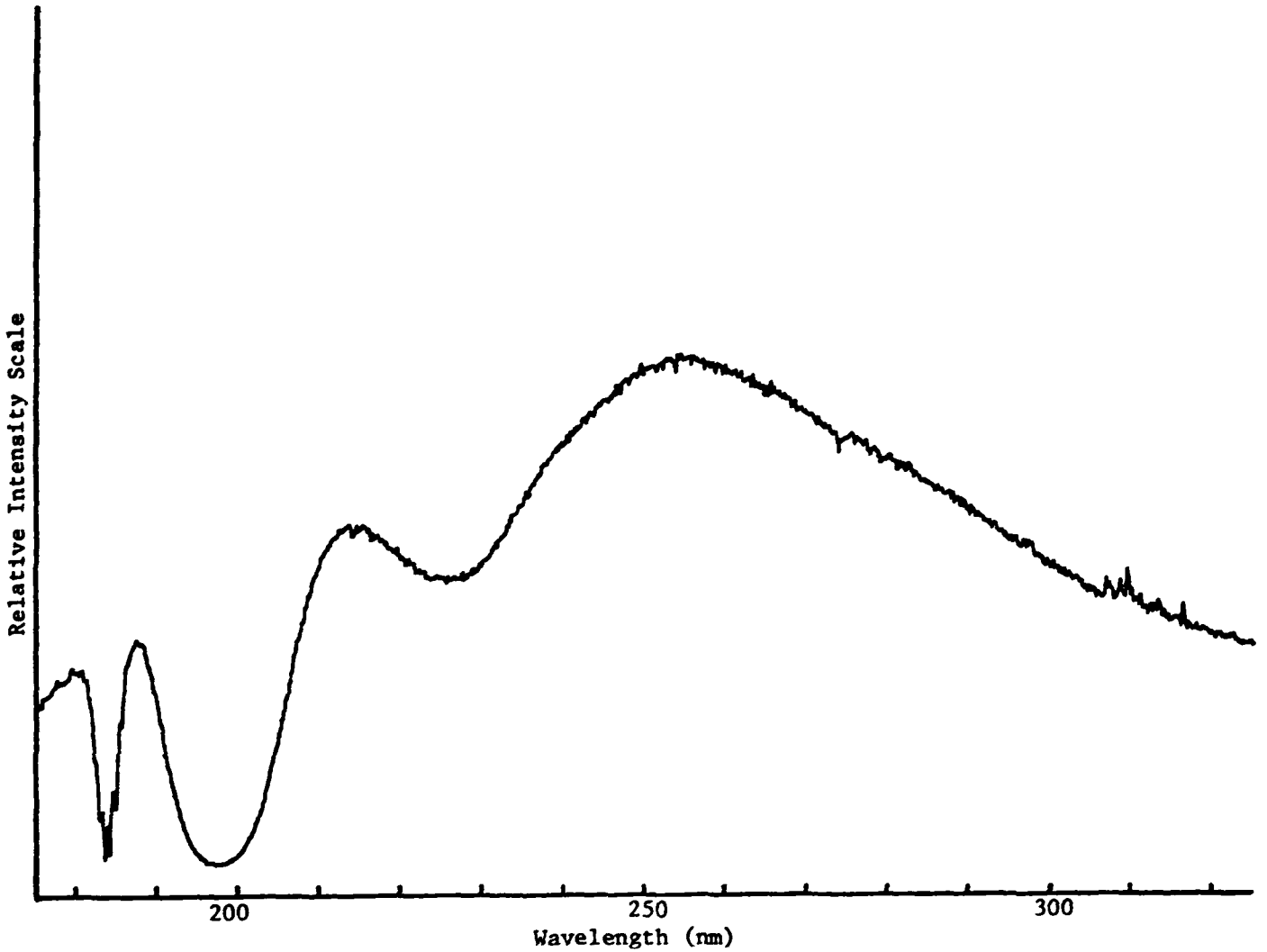

Figure 18: Transmission Spectrum at 128°C

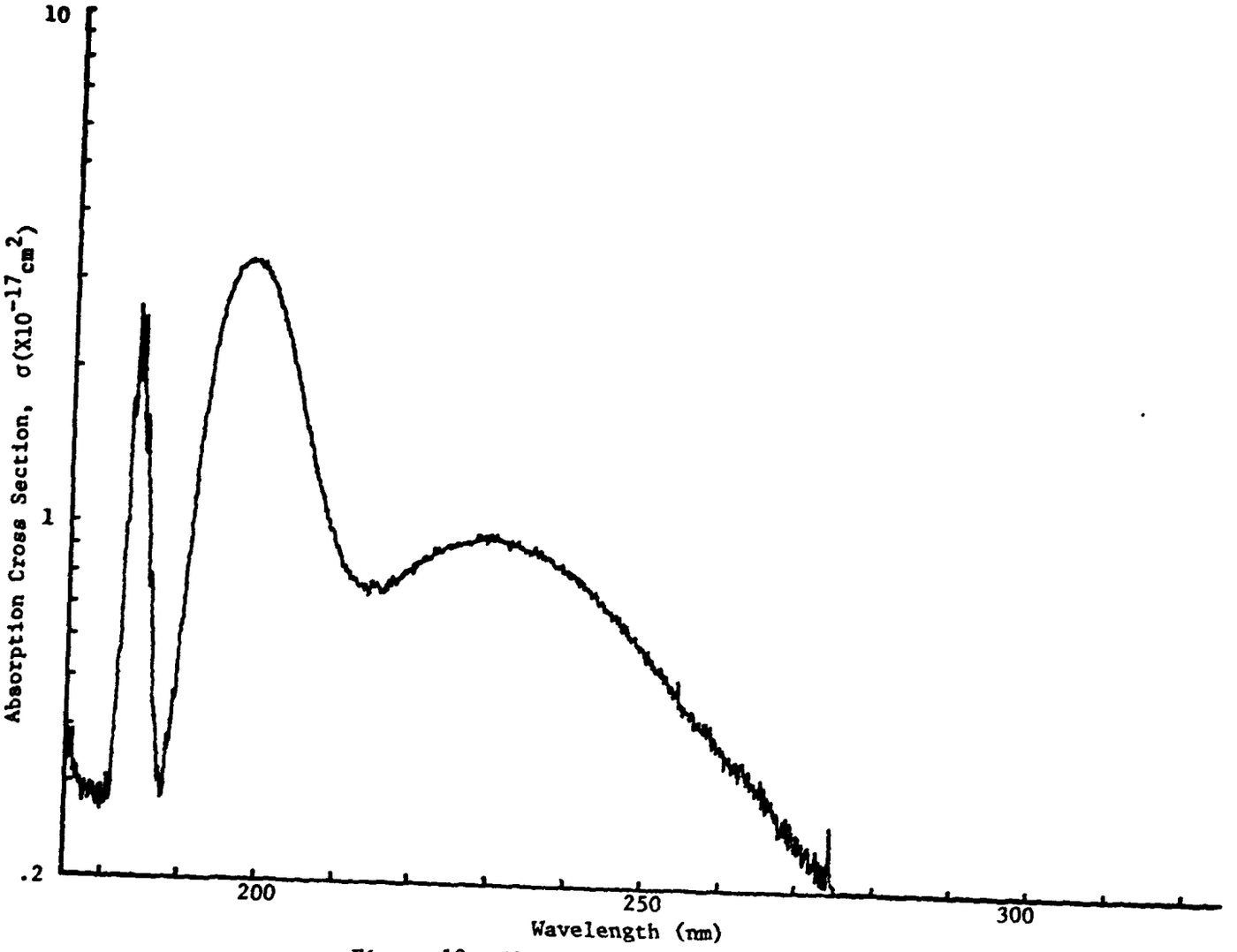

Figure 19: Measured Cross Section at 128°C

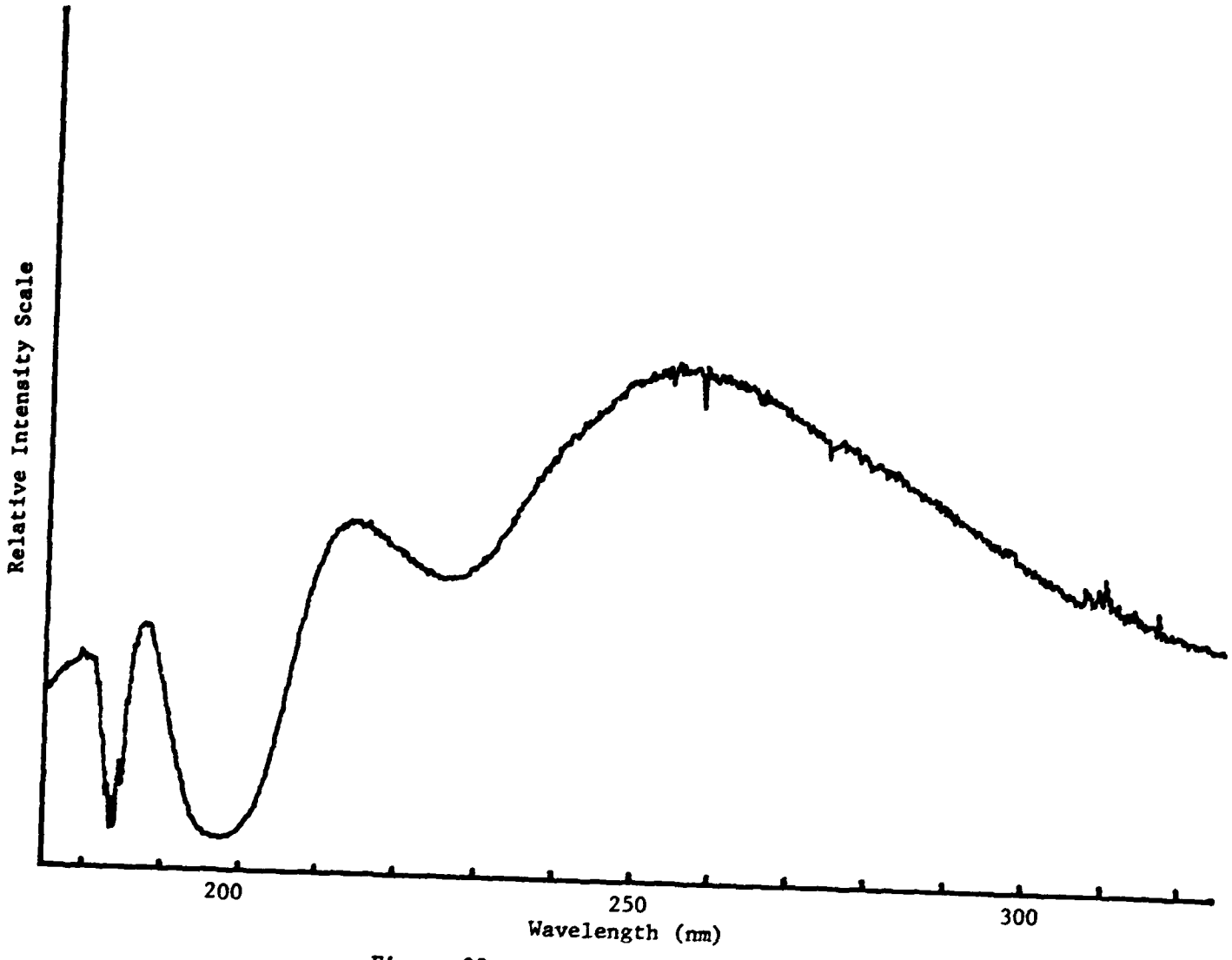

Figure 20: Transmission Spectrum at 129°C

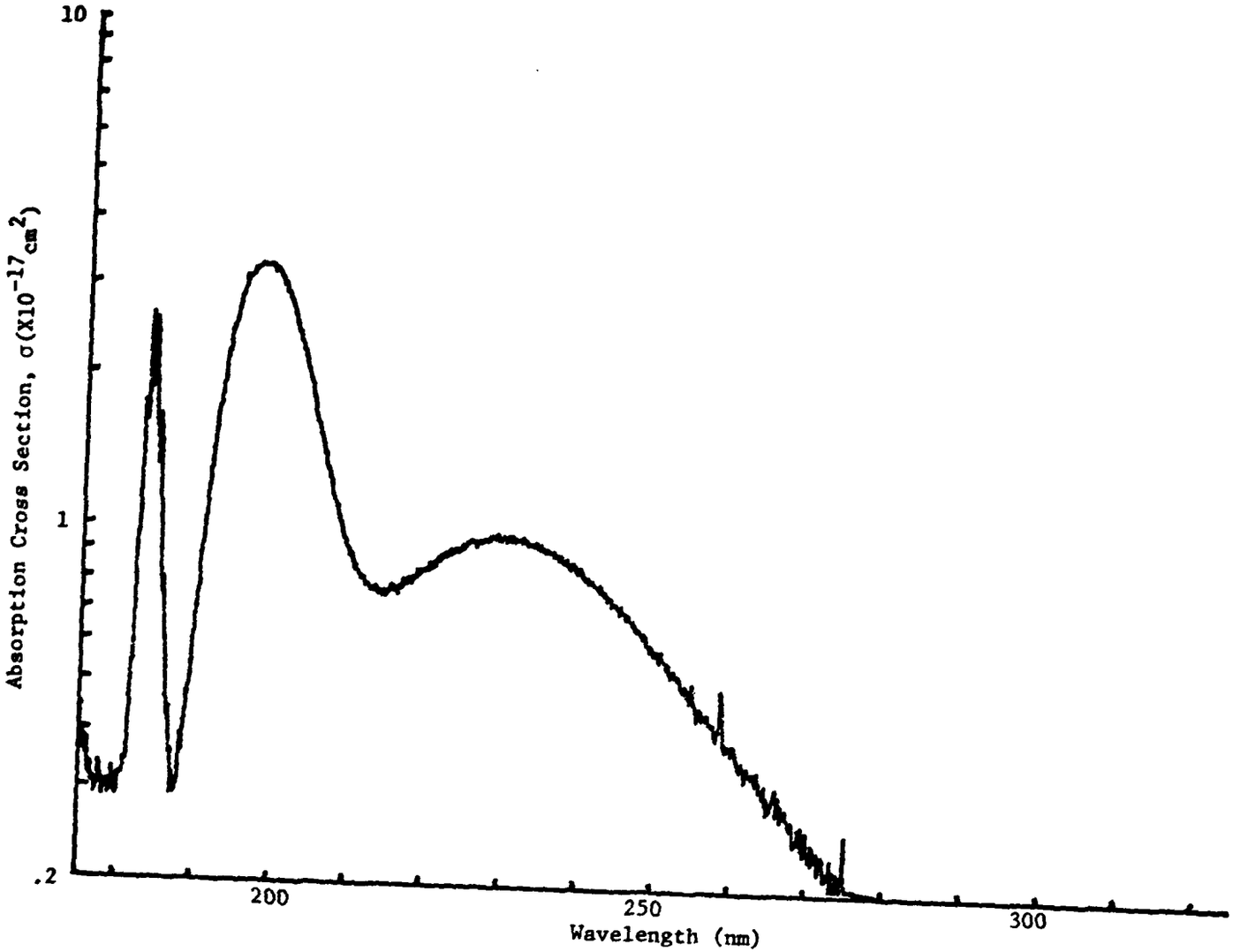

Figure 21: Measured Absorption Cross Section at 129°C

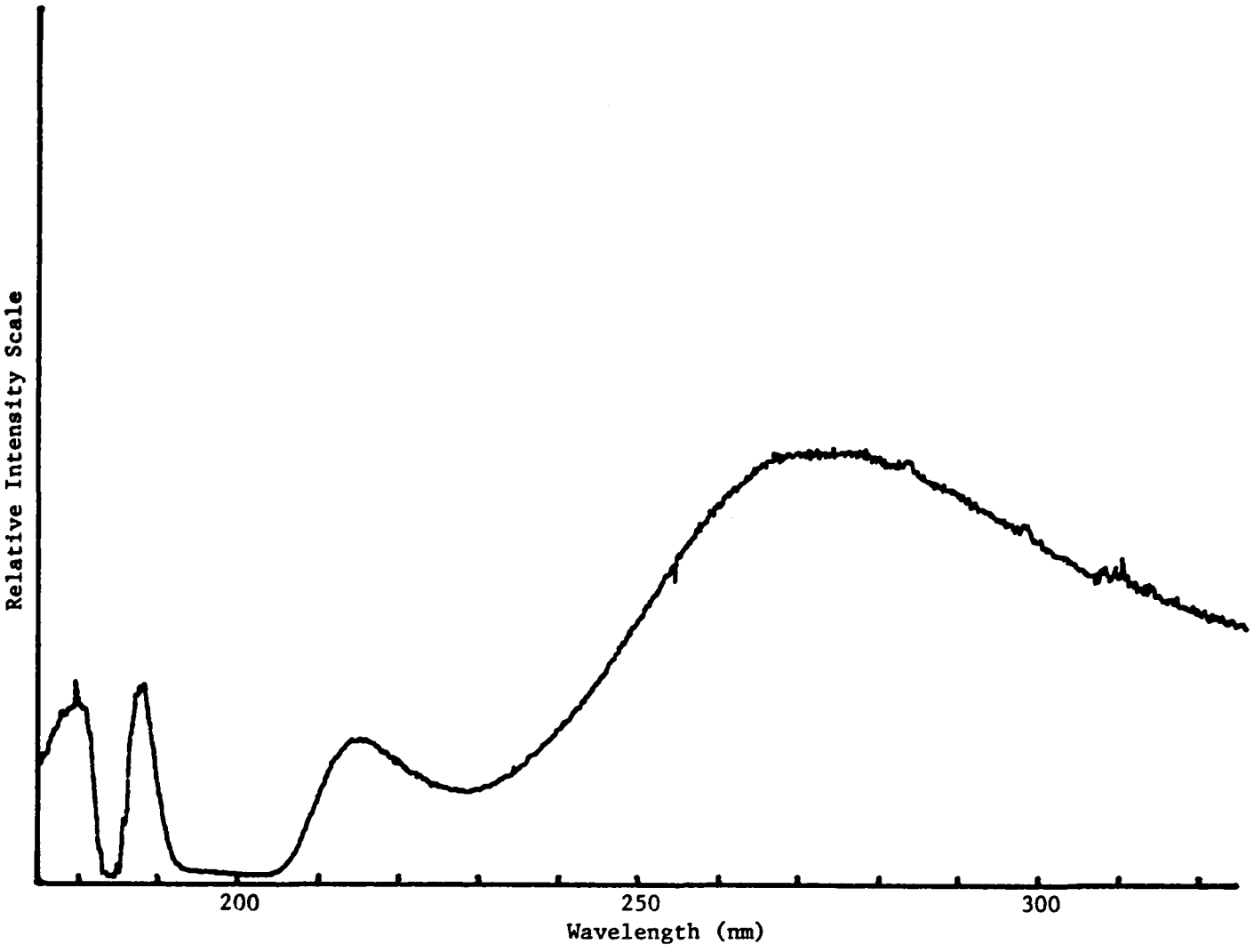

Figure 22: Transmission Spectrum at 151°C

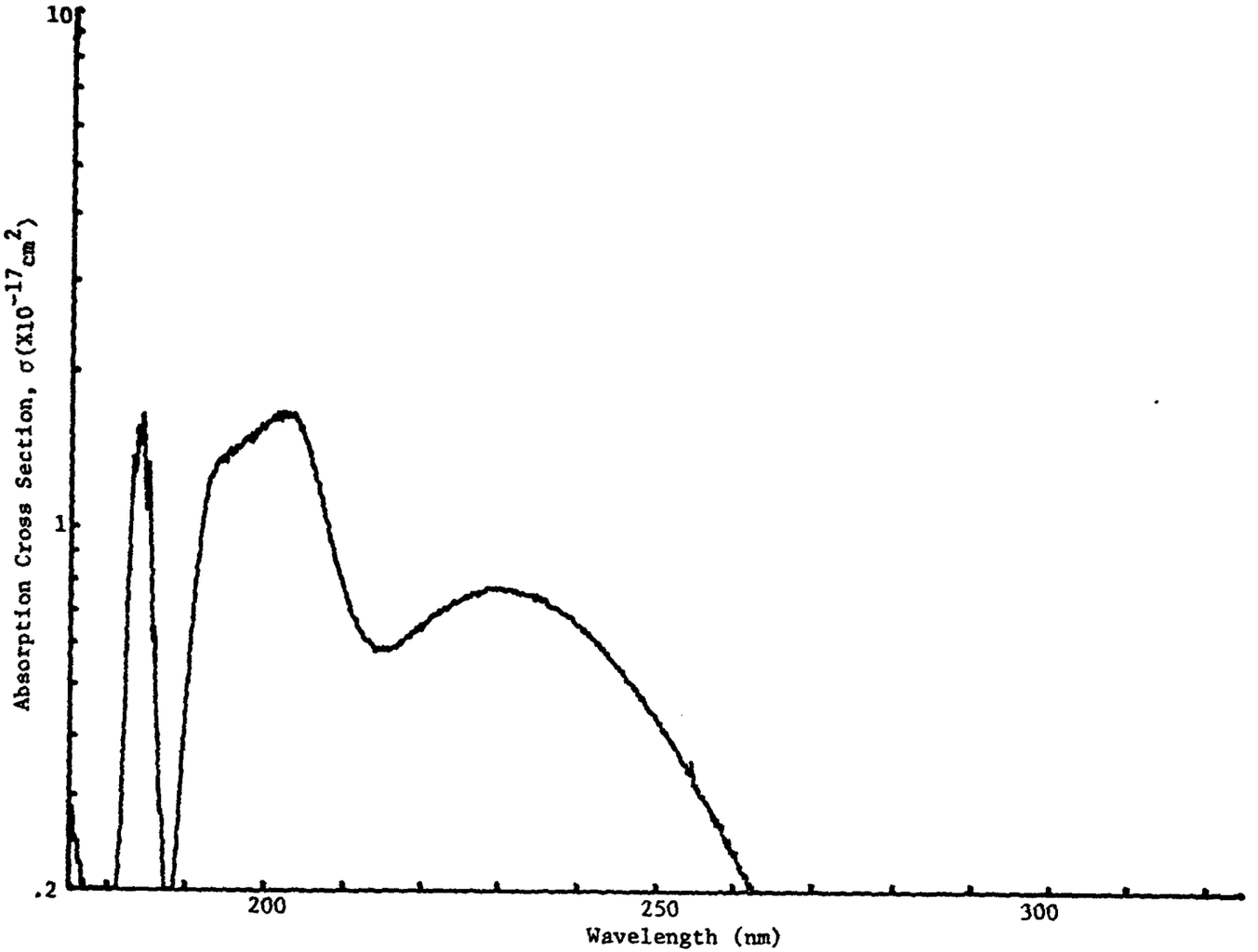

Figure 23: Measured Absorption Cross Section at 151°C

APPENDIX B

Calculations of Noise Caused by the HgBr Fluorescence

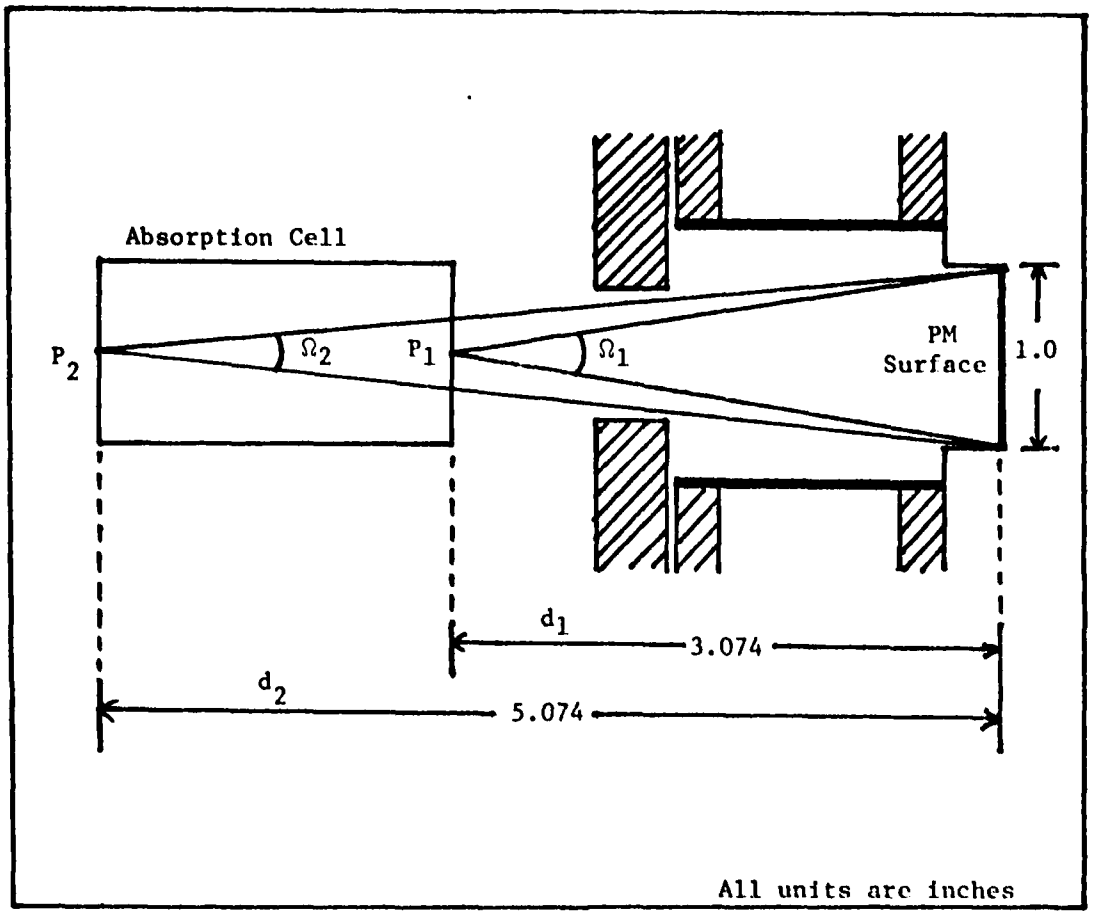

Figure 24: Diagram for Fluorescent Noise Calculations

Find surface area produced by Ω_1 (S_1):

$$R_1 = [(\tfrac{1}{2})^2 + (3.074)^2]^{\frac{1}{2}}$$

$$= 3.1144 \text{ in}$$

$$S_1 = 2\pi R_1(R_1 - d_1) = 2\pi(3.1144\ \text{in})(3.1144\ \text{in} - 3.074\ \text{in})$$

$$= 2\pi(3.1144\ \text{in})(0.0404\ \text{in})$$

$$\boxed{S_1 = 0.7906\ \text{in}^2}$$

Find surface area produced by Ω_2 (S_2):

$$R_2 = [(5)^2 + (5.074)^2]^{\frac{1}{2}}$$

$$= 5.0986\ \text{in}$$

$$S_2 = 2\pi R_2(R_2 - d_2) = 2\pi(5.0986\ \text{in})(5.0986\ \text{in} - 5.074\ \text{in})$$

$$= 2\pi(5.0986\ \text{in})(0.0246\ \text{in})$$

$$\boxed{S_2 = 0.7881\ \text{in}^2}$$

Find Ω_1:

$$\Omega_1 = S_1/R_1^2 = 0.7906\ \text{in}^2/(3.1144\ \text{in})^2$$

$$\boxed{\Omega_1 = 0.0815\ \text{st. rad.}}$$

Find Ω_2:

$$\Omega_2 = S_2/R_2^2 = 0.7881\ \text{in}^2/(5.0986\ \text{in})^2$$

$$\boxed{\Omega_2 = 0.0303\ \text{st. rad.}}$$

If the fluorescent light is isotropic, then it will be evenly distributed over a 4π st. rad. solid angle.

So:

$$\text{Percent of light in } \Omega_1 \equiv L_1 = \Omega_1/4\pi \times 100\%$$

$$= 0.0815/4\pi \times 100\%$$

$$\boxed{L_1 = 0.649\%}$$

And:

$$\text{Percent of light in } \Omega_2 \equiv L_2 = \Omega_2/4\pi \times 100\%$$

$$= 0.0303/4\pi \times 100\%$$

$$\boxed{L_2 = 0.241\%}$$

Analysis

Even if the quantum efficiency is 100%, the amount of fluorescent light that will strike the photomultiplier is so small (<1%) that it will be covered, or masked-over, by the background noise.

Example

Define:

T = Fraction of transmitted light

I = Input intensity

A = Intensity of absorbed light

QE = Efficiency of fluorescence

L = Percentage of fluorescence to reach PM

Ideal absorption (no fluorescence):

$$T = \frac{I-A}{I} = 1 - \frac{A}{I} \equiv T_o$$

Introduce quantum efficiency:

$$T = \frac{I - A(1 - QE)}{I} = 1 - \frac{A}{I}(1 - QE) = T_o + \frac{A}{I} QE$$

If QE is significant, then the fluorescence is significant. But the fact that not all the fluorescent light will reach the PM must be introduced. Then:

$$T = \frac{I - A[1 - QE(L)]}{I}$$

$$= 1 - \frac{A}{I}[1 - QE(L)]$$

$$= T_o + \frac{A}{I}[QE(L)]$$

If the last term, $\frac{A}{I}[QE(L)]$, can be shown to be small, then it can be ignored.

If there is 100% absorption, $T_o = 0$, and $A = I$. This will produce the largest value of $\frac{A}{I}[QE(L)]$ for the system. Assuming that full scale deflection is caused when $T = I$ (i.e. $A = 0$ and $T_o = I$), then what deflection will be caused by $A = I$?

A good approximation of the best QE for $HgBr_2$ is ~25% and the maximum value for L was computed to be ~0.65%. Using these numbers one obtains

$$QE(L) = 0.25(0.0065)$$

$$= 1.625 \times 10^{-3}$$

$$= 0.1625\%$$

Or, the maximum error introduced by the fluorescent light will be on the order of 0.1625% of full scale.

APPENDIX C

Oven Drawings

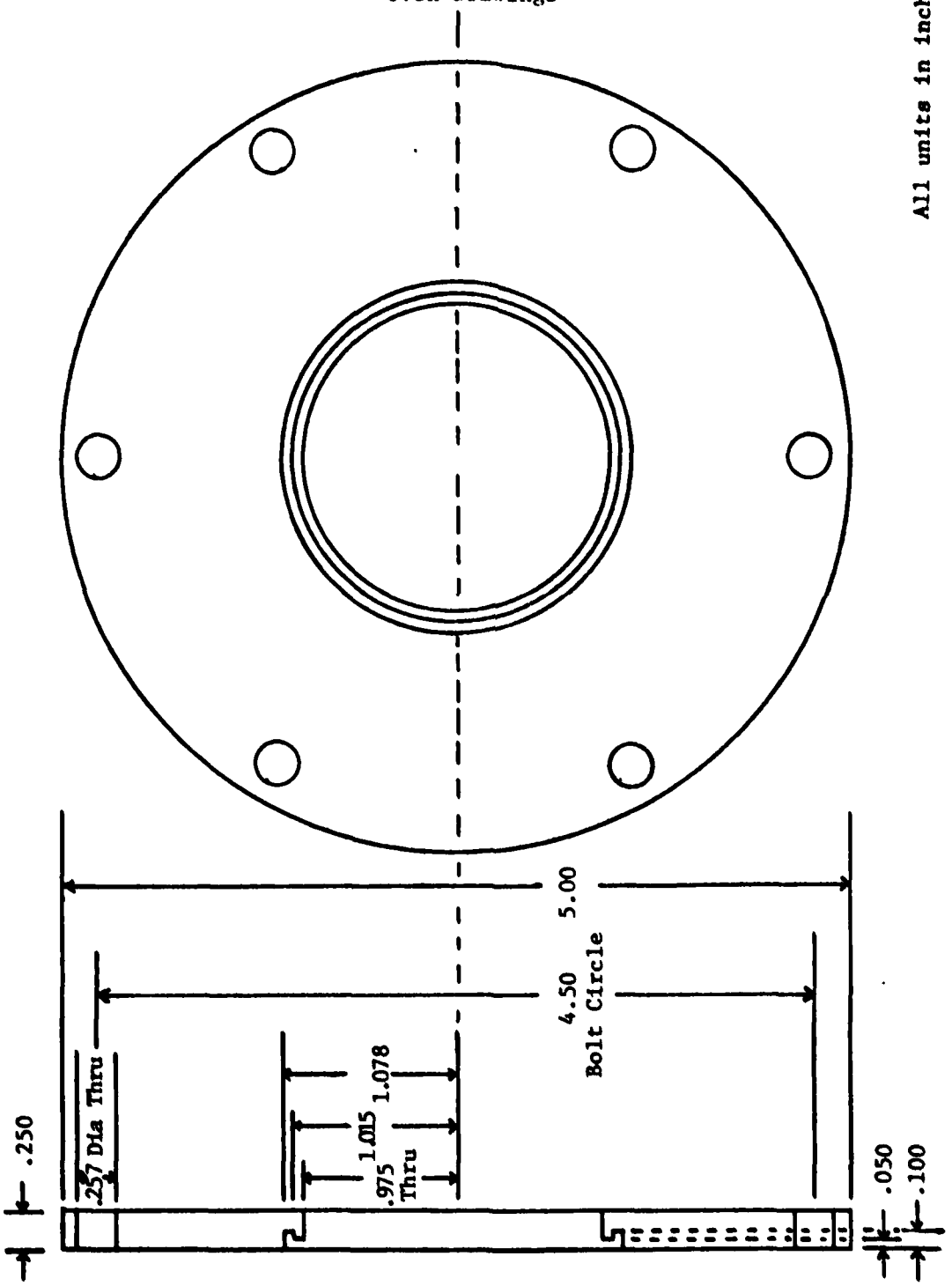

All units in inches

Figure 25: Oven Flange #1 (#304 Stainless Steel)

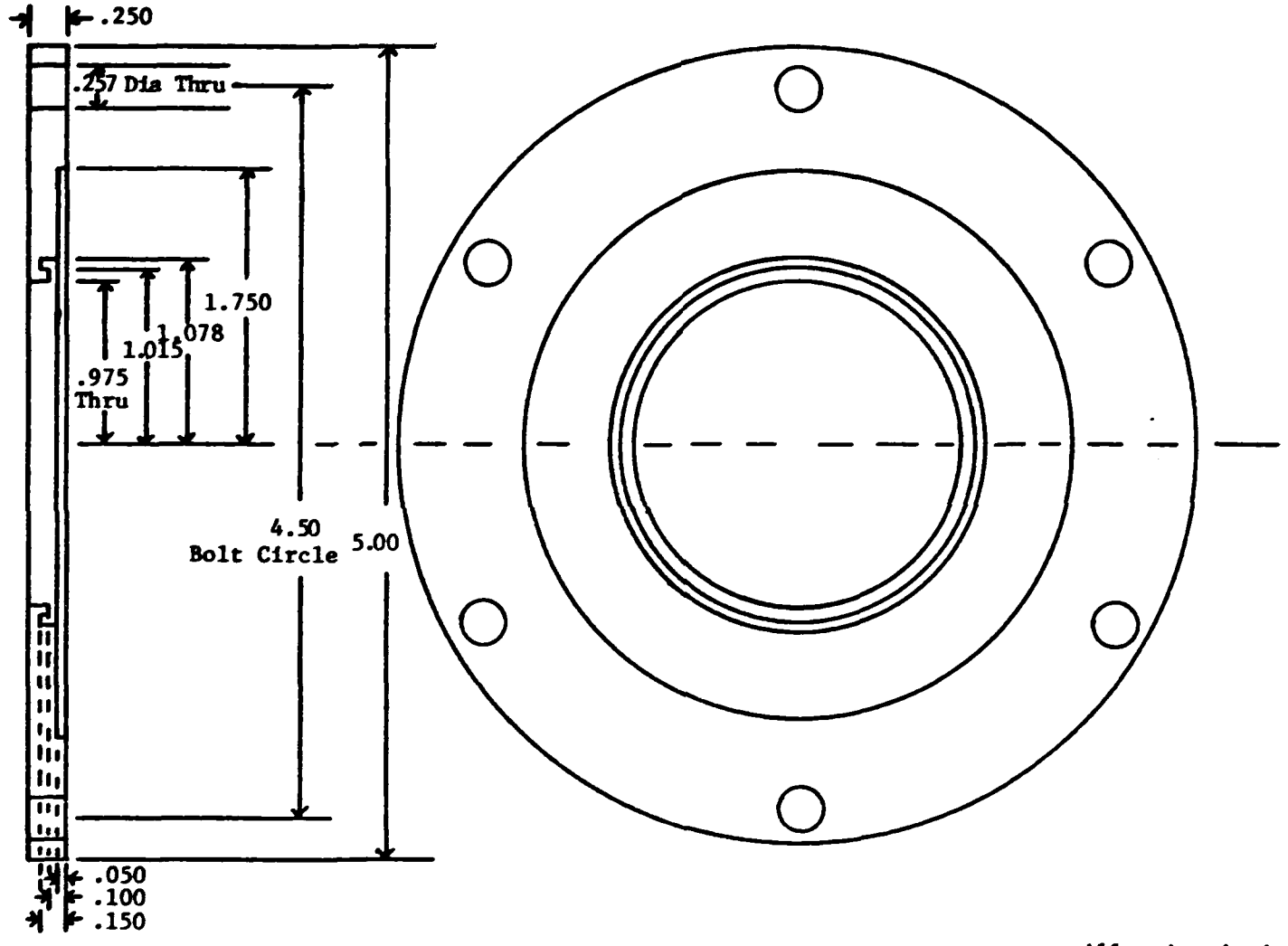

All units in inches

Figure 26: Oven Flange #2 and #5 (#304 Stainless Steel)

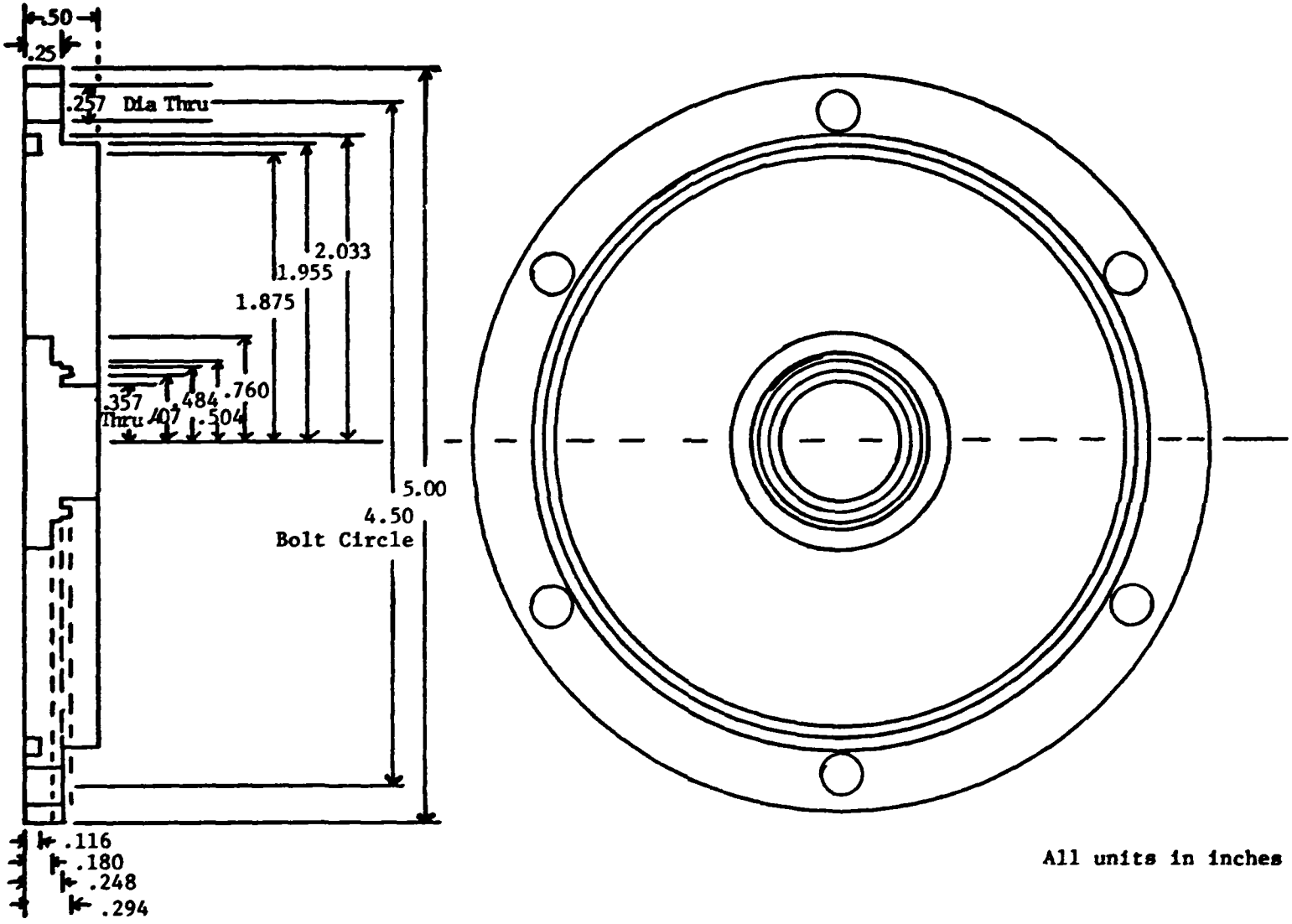

Figure 27: Oven Flange #3 (#6061 Aluminum)

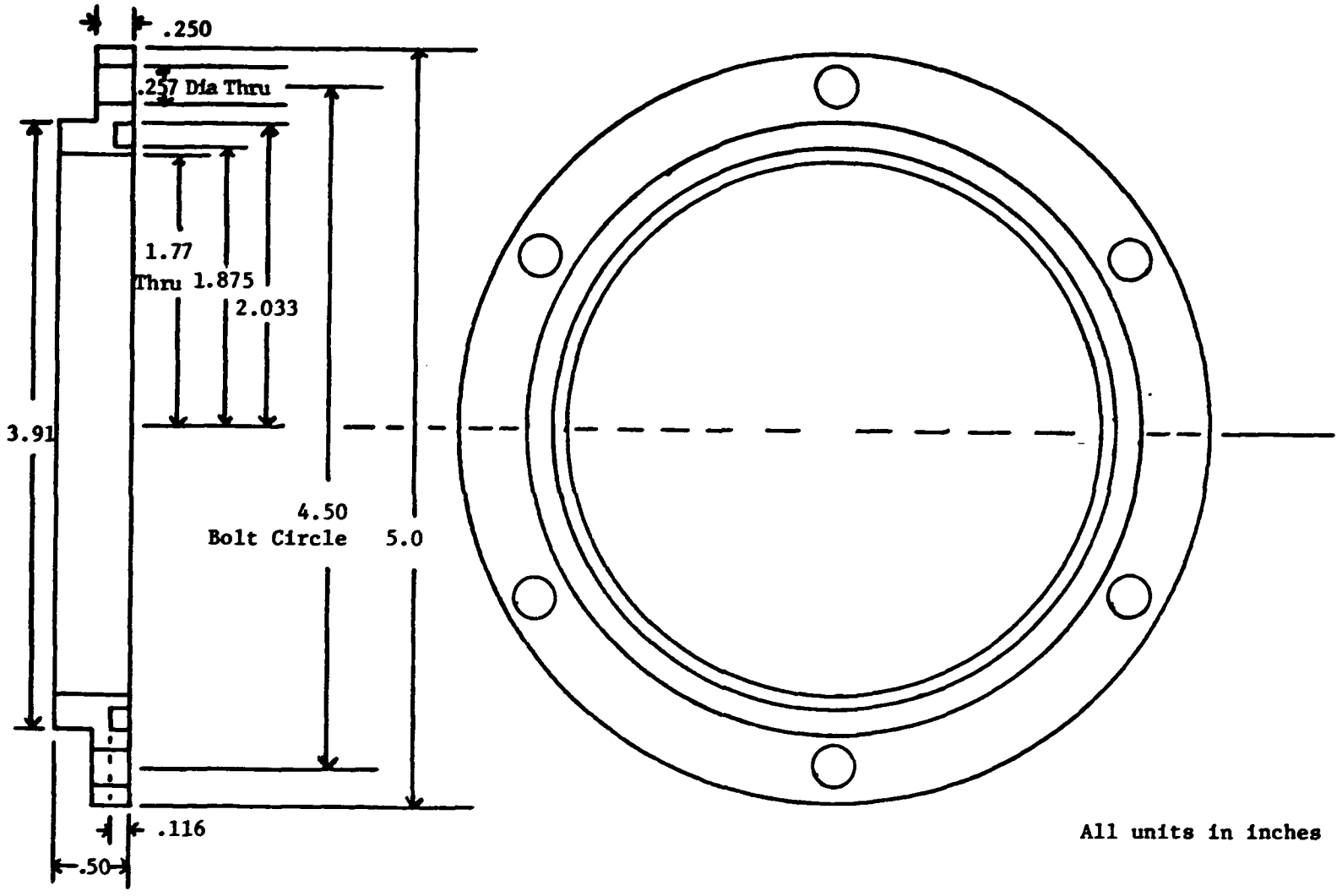

Figure 28: Oven Flange #4 (#6061 Aluminum)

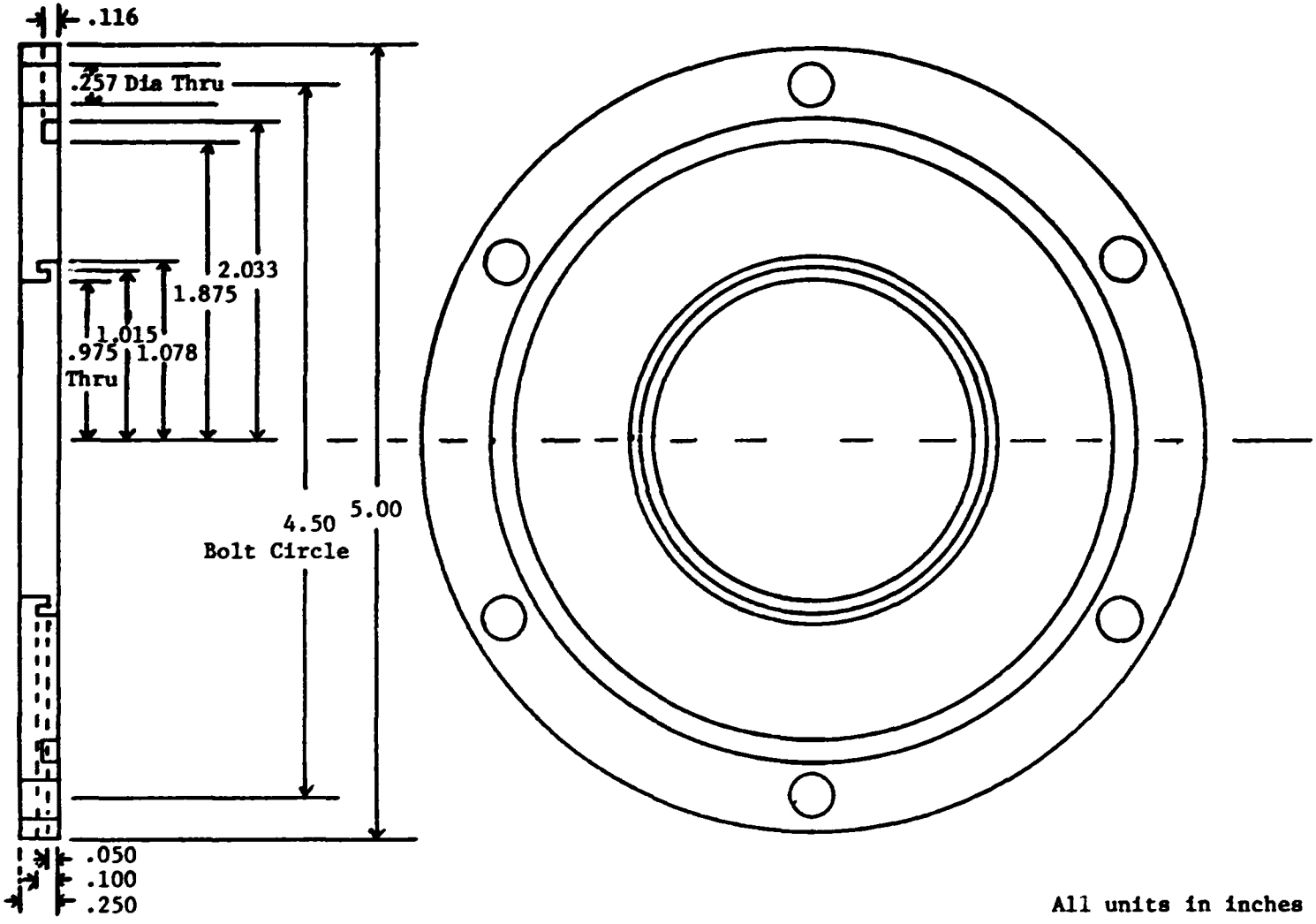

Figure 29: Oven Flange #6 (#304 Stainless Steel)

APPENDIX D

Computer Program

```
      PROGRAM ABSPT
C  SET UP BUFFER TRANSFER
      CALL BUFER (NP,RANG1,RANG2)
C
C  OPERATION SELECTION ON SWITCH REGISTER
C
C   ASSUME DATA ALREADY IN MEMORY
C   ABSORPTION COEFFICIENT PLOT CHECK
10    IF (ISSW(1)) 400,20
C   RAW DATA PLOT CHECK
20    IF (ISSW(3)) 500,30
C   PUNCH CHECK
30    IF (ISSW(4)) 600,40
C   DATA INPUT MODE CHECK
40    IF (ISSW(11)) 300,50
C   DATA CATEGORY CHECK
50    IF (ISSW(6)) 100,200
C   RETURN POINT AFTER SCAN
70    IF (ISSW(15)) 80,90
80    WRITE (2,1000)
1000  FORMAT (/"SCAN ABORTED")
90    PAUSE
      GO TO 10
C
C  REAL-TIME BACKGROUND SPECTRA ENTRY
C
100   IBFLG=1
      WRITE (2,1100)
1100  FORMAT (3/"ENTER DATE")
      READ (1,1110) NUM1A,NUM1B
1110  FORMAT (2I3)
      WRITE (2,1120)
1120  FORMAT (/"ENTER: RUN NUMBER"/7X"NUMBER OF POINTS,
     * TIME PER POINT"/7X"GAIN")
      READ (1,*) NUM1C
      READ (1,*) NP,T
      IT=10.*T
      READ (1,*) GAIN1
      RANG1=1./GAIN1
      CALL BSCAN (IT,NP,GAIN1,IERR)
      GO TO 70
C
C  REAL-TIME ABSORPTION SPECTRA ENTRY
C
200   IF (IBFLG) 210,220
210   WRITE (2,1210)
1210  FORMAT (/"BACKGROUND NOT LOADED")
      GO TO 90
```

```
220   WRITE (2,1220) NP
1220  FORMAT (/"NUMBER OF POINTS ="I0/"ENTER: DATE"/7X
     *"RUN NUMBER"/7X"TIME PER POINT"/7X"GAIN")
      READ (1,1110) NUM2A,NUM2B
      READ (1,*) NUM2C
      READ (1,*) T
      IT=10.*T
      READ (1,*) GAIN2
      RANG2=1./GAIN2
      CALL ASCAN (IT,NP,GAIN2,IERR)
      GO TO 70
C
C  PAPER TAPE DATA ENTRY
C
300   IF (ISSW(6)) 310,320
310   IBFLG=1
      CALL TAPIN (NUM1A,NUM1B,NUM1C,NP,GAIN1,GAIN2)
      RANG1=1./GAIN1
      WRITE (2,1300)
1300  FORMAT (/"BACKGROUND -")
      WRITE (2,1320) NUM1A,NUM1B,NUM1C,NP,GAIN1
      GO TO 90
320   IF (IBFLG) 330,340
330   WRITE (2,1210)
      GO TO 90
340   CALL TAPIN (NUM2A,NUM2B,NUM2C,NP,GAIN1,GAIN2)
      RANG2=1./GAIN2
      WRITE (2,1310)
1310  FORMAT (/"ABSORPTION -")
      WRITE (2,1320) NUM2A,NUM2B,NUM2C,NP,GAIN2
1320  FORMAT ("DATA ENTERED"/"RUN NO. "2I5"-"I3/I4" POINTS"
     */"GAIN ="E9.3)
      GO TO 90
C
C  PLOT ABSORPTION CROSS SECTION
C
400   WRITE (2,1400)
1400  FORMAT (/"ENTER TEMPERATURE (DEG C), PATH LENGTH")
      READ (1,*) TEMP,PATH
      P=10.**((-0.2185*19072.7/(TEMP+273.15))+10.181)
      IF (ISSW(5)) 410,420
410   WRITE (2,1415)
1415  FORMAT (/"ENTER PRESSURE")
      READ (1,*) PRESS
      P=PRESS
420   DENS=(0.269E20/760.0)*P/(1.0+TEMP/273.15)
      YMULT=1.0/(DENS*PATH)
      YMIN=ALOG(CUR1(1)/CUR2(1))*YMULT
      YMAX=YMIN
      DO 460 I=2,NP
      Y=ALOG(CUR1(I)/CUR2(I))*YMULT
      IF (Y-YMAX) 430,440
430   IF (Y-YMIN) 450,460
440   YMAX=Y
```

```
      GO TO 460
450   YMIN=Y
460   CONTINUE
      WRITE (2,1470) YMIN,YMAX
1470  FORMAT (/"Y-MIN ="E8.2,3X"Y-MAX ="E8.2/
     *"ENTER Y-MIN, Y-MAX")
      READ (1,*) YMIN,YMAX
      CALL BCAL (NP,X,Y)
      X=9999.0/(FLOAT(NP-1))
      AX=0.0
      YMINL=ALOG(YMIN)
      SCALE=9999.0/(ALOG(YMAX)-YMINL)
      DO 490 I=1,NP
      Y=ALOG(ALOG(CUR1(I)/CUR2(I))*YMULT)
      IX=AX
      IY=(Y-YMINL)*SCALE
      AX=AX+X
490   CALL XYPLT(IX,IY)
      CALL ECAL
      GO TO 90
C
C  PLOT RAW DATA
C
500   CALL OUTPT (NP)
      GO TO 90
C
C  PUNCH RAW DATA
C
600   IF (ISSW(6)) 610,620
610   CALL PDATA (NUM1A,NUM1B,NUM1C,NP,GAIN1)
      GO TO 90
620   CALL PDATA (NUM2A,NUM2B,NUM2C,NP,GAIN2)
      GO TO 90
      END
      END$
```

This is the computer program that was written to control the input, output, and the library. The library software routines were already in existence and had been used previously by D. F. Grosjean (Ref 12). The first section, Operation Selection on Switch Register, is the section where the operator would tell the computer what was being entered or what was wanted for an output. The 16 switches on the front of the computer would be tested, by the computer, to see if they were up or down. The following is a table of switch operations for this program.

Table I: Switch Settings for Absorption Program

Function	Switch # Up
1. Enter background data	
Real time	6
Paper tape	11, 6
2. Enter Transmission data	
Real time	(All down)
Paper tape	11
3. Real time raw data plot of background	2
4. Raw data plot (after data has been entered)	
Background	3, 6
Transmission	3
5. Compute and plot absorption cross-section	1
Manual override (to enter pressure)	1, 8
6. Punch data onto paper tape	
Background	4, 6
Transmission	4
7. Verify data (in conjunction with punch)	
Background	5, 6
Transmission	5
8. Abort scan (at any time)	15
9. Free run of equipment without scan	14

In Table I, if a switch is not mentioned for a particular step, then it must be in the down position, otherwise it might interrupt the proposed operation.

The second section, Real-Time Background Spectra Entry, was used to record the signal from the DVM and to store it for later use. The third section, Real-Time Absorption Spectra Entry, is the same as the background entry, only the computer would store it separate of the background. The fourth section, Paper Tape Data Entry, has the computer take raw data from the paper tape previously punched (last section) and store it as background

or transmission spectra depending on the position of switch #6 (See Table I).

The next section, Plot Absorption Cross Section, computed the absorption cross-section from the background and transmission data, the computer would compute the vapor pressure from the given temperature unless switch #8 was up, then the pressure would be entered manually. The next section, Plot Raw Data, would have the computer send the stored information, background or transmission, to the x-y plotter. And, the last section, Punch Raw Data, would have the computer send a copy of the raw data, background or transmission, to the paper tape punch for storage for later use.

Vita

Gordon L. Frantom was born on 11 August 1953 in Troy, Ohio. He is the son of Mr. and Mrs. Marvin D. Frantom of Ft. Myers, Florida. He graduated from Ft. Myers Senior High School, Ft. Myers, Fl. in 1971. He graduated from Edison Community College, Ft. Myers, Fl. in 1976 and from the University of Florida, Gainesville, Fl. in 1978. His first assignment in the USAF was in June 1978 when he entered the Air Force Institute of Technology.

Permanent Address: 2610 Elmwood
Ft. Myers, Fl. 33901

This Thesis was typed by Jill Rueger.

Unclassified

SECURITY CLASSIFICATION OF THIS PAGE (When Data Entered)

REPORT DOCUMENTATION PAGE		READ INSTRUCTIONS BEFORE COMPLETING FORM
1. REPORT NUMBER AFIT/GEP/PH/79D-2	2. GOVT ACCESSION NO.	3. RECIPIENT'S CATALOG NUMBER
4. TITLE (and Subtitle) ULTRAVIOLET ABSORPTION CROSS SECTION OF MERCURIC BROMIDE		5. TYPE OF REPORT & PERIOD COVERED MS Thesis 6. PERFORMING ORG. REPORT NUMBER
7. AUTHOR(s) Gordon L. Frantom, 2Lt, USAF		8. CONTRACT OR GRANT NUMBER(s)
9. PERFORMING ORGANIZATION NAME AND ADDRESS Air Force Institute of Technology (AFIT-EN) Wright-Patterson AFB, Ohio 45433		10. PROGRAM ELEMENT, PROJECT, TASK AREA & WORK UNIT NUMBERS
11. CONTROLLING OFFICE NAME AND ADDRESS Air Force Wright Aeronautical Laboratories (AFAPL/POE-3) Wright-Patterson AFB, Ohio 45433		12. REPORT DATE December, 1979 13. NUMBER OF PAGES 68
14. MONITORING AGENCY NAME & ADDRESS(if different from Controlling Office)		15. SECURITY CLASS. (of this report) Unclassified 15a. DECLASSIFICATION DOWNGRADING SCHEDULE

16. DISTRIBUTION STATEMENT (of this Report)

Approved for public release; distribution unlimited.

17. DISTRIBUTION STATEMENT (of the abstract entered in Block 20, if different from Report)

18. SUPPLEMENTARY NOTES Approved for public release; IAW AFR 190-17

JOSEPH P. HIPPS, Major, USAF
Director of Public Affairs

19. KEY WORDS (Continue on reverse side if necessary and identify by block number)

Ultraviolet Absorption
Vacuum Ultraviolet Absorption
Mercury Halides
Mercuric Bromide

20. ABSTRACT (Continue on reverse side if necessary and identify by block number)

This report is on the measurements of the ultraviolet absorption cross section of mercuric bromide ($HgBr_2$) from 175.0 nm to 325.0 nm and discusses the need for such measurements. The ultraviolet radiation wavelengths from a hydrogen discharge lamp were selected by a vacuum monochromator (0.25 nm resolution) and passed through an absorption cell, made of fused quartz, containing the $HgBr_2$. The experiments were conducted over the temperature range 110°C to 150°C corresponding to vapor pressures of 0.2 torr to 2.15 torr of the $HgBr_2$. The results of this study are compared with the results of previous studies and

DD FORM 1 JAN 73 1473 EDITION OF 1 NOV 65 IS OBSOLETE Unclassified

SECURITY CLASSIFICATION OF THIS PAGE (When Data Entered)

clears up several discrepancies concerning the value of the absorption cross section. If further measures the value of the cross section of an absorption band at 184 nm that was not previously available.